TOPICAL REVIEW

Quark-Gluon Matter

David d'Enterria

CERN, PH-EP, CH - 1211 Geneva 23, Switzerland

E-mail: e-mail:david.d'enterria@cern.ch

Abstract. A concise review of the experimental and phenomenological progress in high-energy heavy-ion physics over the past few years is presented. Emphasis is put on measurements at BNL-RHIC and CERN-SPS which provide information on fundamental properties of QCD matter at extreme values of temperature, density and low-x. The new opportunities accessible at the LHC, which may help clarify some of the current open issues, are also outlined.

PACS numbers: 12.38.-t, 12.38.Mh, 13.85.-t, 13.87.Fh, 25.75.-q, 25.75.Nq

Introduction

The study of the fundamental theory of the strong interaction – Quantum Chromo Dynamics (QCD) – in extreme conditions of temperature, density and small parton momentum fraction (low-x) has attracted an increasing experimental and theoretical interest during the last 20 years. Indeed, QCD is not only a quantum field theory with an extremely rich dynamical content (asymptotic freedom, infrared slavery, (approximate) chiral symmetry, non trivial vacuum topology, strong CP violation problem, $U_A(1)$ axial-vector anomaly, ...) but also the only sector of the Standard Model whose full *collective* behaviour – phase diagram, phase transitions, thermalization of fundamental fields – is accessible to scrutiny in the laboratory. The study of the many-body dynamics of high-density QCD covers a vast range of fundamental physics problems (Fig. 1):

- **Deconfinement and chiral symmetry restoration**: Lattice QCD calculations [1] predict a new form of matter at energy densities (well) above $\varepsilon_{crit} \approx 1$ GeV/fm^3 consisting of an extended volume of deconfined and bare-mass quarks and gluons: the Quark Gluon Plasma (QGP) [2]. The scrutiny of this new state of matter – equation-of-state (EoS), order of the phase transition, transport properties, etc. – promises to shed light on basic aspects of the strong interaction such as the nature of confinement, the mechanism of mass generation (chiral symmetry breaking, structure of the QCD vacuum) and hadronization, which still evade a thorough theoretical description [3] due to their highly non-perturbative nature.
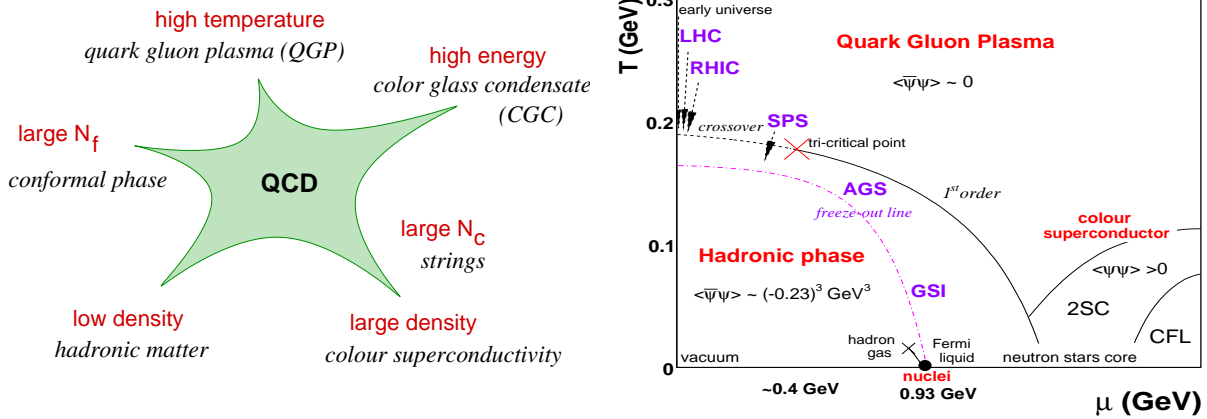
Figure 1. Left: The multiple facets of QCD (adapted from [4]). Right: QCD phase diagram in the temperature vs. baryochemical potential (T, μ_B) plane. The arrows indicate the expected crossing through the deconfinement transition during the expansion phase in heavy-ion collisions at different accelerators. The dashed freeze-out curve indicates where hadrochemical equilibrium is attained in the latest stage of the collision [5].

- **Early universe cosmology**: The quark-hadron phase transition took place some $10\ \mu s$ after the Big-Bang and is believed to have been the most important event in the Universe between the electro-weak (or SUSY) transition ($\tau \sim 10^{-10}$ s) and nucleosynthesis ($\tau \sim 200$ s). Depending on the order of the transition‡, several cosmological implications have been postulated [6] such as the formation of strangelets and cold dark-matter (WIMP) clumps, or baryon fluctuations leading to inhomogeneous nucleosynthesis.

- **Parton structure and evolution at small-x**: HERA data [7] indicate that when probed at high energies, hadrons consist of a very dense system of gluons with small (Bjorken) momentum $x = p_{parton}/p_{hadron}$. At low x, the probability to emit an extra gluon is large, proportional to $\alpha_s \ln(1/x)$, and gg fusion processes will play an increasing role in the parton evolution in the hadronic wavefunctions. At high virtualities Q^2 and moderately low x, such evolution is described by linear DGLAP [8] or BFKL [9] equations, suitable for a dilute parton regime. At $x \lesssim 10^{-2}$ and below an energy-dependent "saturation momentum" Q_s, hadrons are however more appropriately described as dense, saturated parton systems in the context of the "Colour Glass Condensate" (CGC) [10] effective theory with the corresponding non-linear BK/JIMWLK [12, 11] evolution equations. Since the growth of the gluon density depends on the transverse size of the hadron, saturation effects are expected to set in earlier for ultrarelativistic heavy nuclei (for which $Q_s^2 \propto A^{1/3}$, with A the number of nucleons) than for free nucleons.

- **Gauge/String duality**: Theoretical applications of the Anti-de-Sitter/Conformal-Field-Theory (AdS/CFT) correspondence provide results in strongly coupled (i.e. large 't Hooft coupling $\lambda = g^2 N_c \gg 1$) SU(N_c) gauge theories in terms of a weakly-coupled dual gravity

‡ The order itself is not exactly known: the transition, which is 1st-order in pure SU(3) gluodynamics and of a fast cross-over type for $N_f = 2+1$ quarks [1], is still sensitive to lattice extrapolations to the continuum limit.

theory [13]. Recent applications of this formalism for QCD-like ($\mathcal{N} = 4$ super Yang-Mills) theories have led to the determination of transport properties of experimental relevance – such as the QGP viscosity [14], the "jet quenching" parameter $\langle\hat{q}\rangle$ [15], or the heavy-quark diffusion coefficient [16] – from black hole thermodynamics calculations. Such results provide valuable insights on *dynamical* properties of strongly-coupled QCD that cannot be directly treated by perturbative or lattice methods, and open new phenomenological and experimental leads.

- **Compact object astrophysics**: At high baryon densities and not too high temperatures, the attractive force between (colour antisymmetric) quarks can lead to the formation of bound $\langle qq\rangle$ Cooper pairs. Cold dense matter is thus expected to behave as a colour super-conductor with a non trivial quark pairing structure due to the combination of the various quantum numbers involved (spin, colour, flavour) [17]. This regime, currently beyond the direct reach of accelerator-based research (except indirectly in the region of baryon densities around the QCD tri-critical point, Fig. 1 right), may be realised in the core of compact (neutron, hybrid or other exotic) stars and, thus, open to study through astronomical observation.

The only experimental means available so far to investigate the (thermo)dynamics of a multi-parton system involves the use of large atomic nuclei collided at ultrarelativistic energies. Figure 2 left, shows the total center-of-mass energy available for particle production (i.e. subtracting the rest mass of the colliding hadrons) at different accelerators as a function of the first operation year ("Livingston plot") [18]. The exponential increase in performance translates into an energy doubling every 2 (3) years for the ion ($\bar{p}, p$) beams. Head-on collisions of heavy ions (*AA*) can produce extremely hot and dense QCD matter by concentrating a substantial amount of energy ($\mathcal{O}(1\ \mathrm{TeV})$ at mid-rapidities at the LHC, see Fig. 2 right) in an *extended* cylindrical volume $V = \pi R_A^2 \tau_0 \approx 150\ \mathrm{fm}^3$ for a typical large nucleus with radius $R_A = 6.5$ fm, at thermalization times of $\tau_0 = 1$ fm/c.
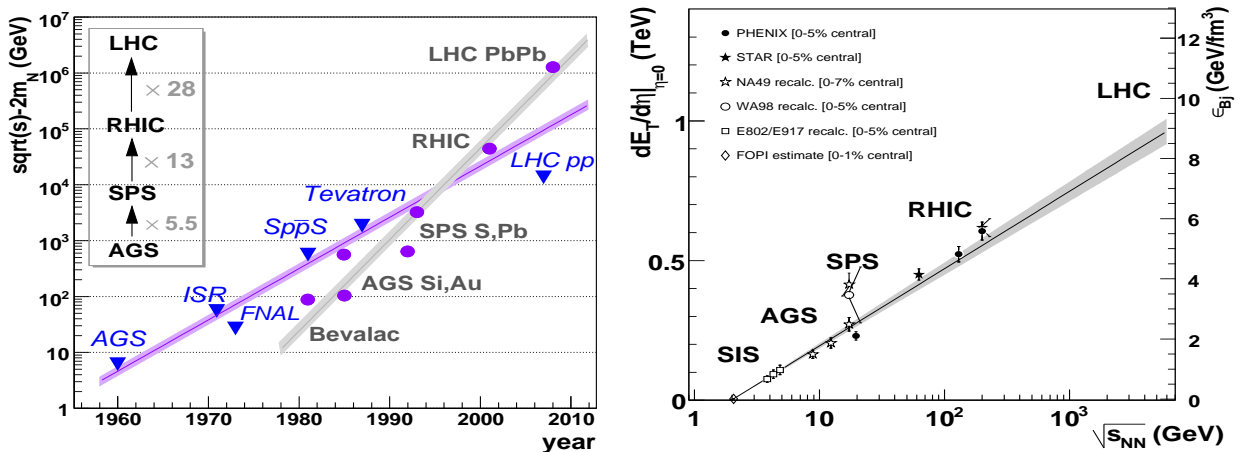

Figure 2. Left: "Livingston plot" for (anti)proton and ion accelerators in the period 1960-2008 (adapted from [18]). Right: Measured transverse energy per unit rapidity at $\eta = 0$, and corresponding Bjorken energy density $\varepsilon_{Bj}(\tau_0 = 1\ \mathrm{fm}/c)$ [19], in central heavy-ion collisions at various c.m. energies [20, 21] fitted to a logarithmic parametrization.

The hot and dense systems produced in high-energy *AA* collisions are not prepared under controlled thermodynamical conditions but they follow a dynamical trajectory along the phase diagram shown e.g. in Fig. 1, right. After the collision, the system (with a temperature profile decreasing from the center) expands with relativistic longitudinal (transverse) velocities $\langle\beta\rangle \approx 1.0(0.5)$ and cools at rates $T \propto \tau^{-1/n}$ (e.g. $n = 3$ for a longitudinal-only expansion [19]). When T reaches $T_{crit} \approx 190$ MeV, the quark matter undergoes a phase transition into hadrons. The produced hadronic gas stops self-interacting collectively at freeze-out times $\tau \approx 10 - 20$ fm/c [22]. At the initial stages of the reaction (1 fm/c after impact), the commonly used "Bjorken estimate" [19] gives energy densities attained at mid-rapidity of $\varepsilon_{Bj} = dE_T/d\eta|_{\eta=0}/(\pi R_A^2 \tau_0) \approx 5, 10$ GeV/fm^3 at RHIC and LHC (Fig. 2 right). Although these values can only be considered as a lower limit since they are obtained in a simple 1+1D expansion scenario ignoring any effects from longitudinal work, they are already about 5 and 10 times larger, respectively, than the QCD critical energy density for deconfinement. High-energy collisions in heavy-ion colliders provide therefore the appropriate conditions for the study of highly excited quark-gluon matter.

This review is organised as follows. Sections 1 introduces the experimental probes of subhadronic matter used in high-energy *AA* collisions. Section 2 briefly reviews the experimental apparatus used in heavy-ion collisions at RHIC and SPS. In Section 3 various hard QCD results from proton-proton collisions at RHIC are presented as the "free space" baseline to which one compares the heavy-ion ("QCD medium") data. Sections 4–11 each discuss a different physics observable in the context of the latest experimental results available at RHIC and SPS. Due to space limitations, the list of topics chosen covers but a fraction of the substantial amount of data collected in the last years. Those observables that provide direct information on the *partonic* phases of the reaction have been given preference over "soft" or bulk observables from the late hadronic stages. Thus, important results relative to the freeze-out phase of the collision – e.g. chemical and kinetic equilibrium from light (and especially strange [23, 24]) hadron abundances [25], "femtoscopy" measurements from HBT radii [26], or possible signatures of (prehadronic) divergent susceptibilities from final net charge and $\langle p_T\rangle$ fluctuations [27] – are not treated here. The selected experimental results are mostly from the comprehensive reviews of the four RHIC experiments (PHENIX [28], STAR [29], PHOBOS [30], and BRAHMS [31]) from *AuAu*, *dAu* and *pp* collisions up to a maximum center-of-mass energy of $\sqrt{s_{NN}} = 200$ GeV, as well as recent results from NA60 *InIn* reactions at SPS ($\sqrt{s_{NN}} = 17.3$ GeV) [32].

1. Experimental probes of QCD matter

Direct information on the thermodynamical and transport properties of the strongly interacting medium produced in *AA* collisions is commonly obtained by comparing the results for a given observable Φ_{AA} to those measured in proton(deuteron)-nucleus ($p(d)A$, "cold QCD matter") and in proton-proton (pp, "QCD vacuum") collisions as a function of c.m. energy, transverse momentum, rapidity, reaction centrality (impact parameter b), and particle type

(mass). Schematically:

$$R_{AA}(\sqrt{s_{NN}}, p_T, y, m; b) \quad = \frac{\text{"hot/dense QCD medium"}}{\text{"QCD vacuum"}} \propto \frac{\Phi_{AA}(\sqrt{s_{NN}}, p_T, y, m; b)}{\Phi_{pp}(\sqrt{s}, p_T, y, m)} \quad (1)$$

$$R_{p(d)A}(\sqrt{s_{NN}}, p_T, y, m; b) = \frac{\text{"cold QCD medium"}}{\text{"QCD vacuum"'}} \propto \frac{\Phi_{p(d)A}(\sqrt{s_{NN}}, p_T, y, m; b)}{\Phi_{pp}(\sqrt{s_{NN}}, p_T, y, m)} \quad (2)$$

The observed *enhancements* and/or *suppressions* in the $R_{AA,dA}(\sqrt{s_{NN}}, p_T, y, m; b)$ ratios can then be directly linked to the properties of the strongly interacting matter after accounting for a realistic modeling of the space-time evolution of the *AA* expansion process.

Among the observables whose *suppression* is expected to provide information on the produced system, we will discuss:

- The **total particle multiplicity** which, related via local parton-hadron duality [33] to the number of initially produced partons, will be suppressed if the initial parton flux is reduced due to low-x saturation effects in the colliding nuclei [34] (Section 4).

- **High-p_T leading hadrons** are expected to be produced in reduced yields due to medium-induced energy loss via gluonsstrahlung of the parent partons in a system with a large number density of colour charges [35, 36] (Sections 6 and 7).

- Dissociation of the **heavy quarkonia** bound states has long since proposed [37] as a sensitive signature of Debye screening effects above T_{crit} (Section 10).

- The **mass of light vector mesons** is expected to drop in some scenarios of chiral symmetry restoration [38, 39] which directly link the in-medium meson mass to a temperature- (and baryon density-) dependent chiral condensate: $m_V^\star \propto m_V \cdot \langle \bar{q}q \rangle(T)$ (Section 11).

Likewise, the following observables discussed hereafter are expected to be *enhanced* in a strongly-interacting multi-parton system compared to the results in *pp* collisions:

- The **soft hadron spectra** ($p_T < 2$ GeV/c), both inclusive and relative to the reaction plane, are expected to be boosted due to the development of collective radial and elliptical (hydrodynamical) flows in the early partonic phases of the reaction [22, 40] (Section 5).

- Semihard ($p_T \approx 2$–5 GeV/c) **yields and flows of baryons** are predicted to be enhanced in the context of parton recombination (or coalescence) models [41] which take into account modifications of the hadronization process in a dense deconfined medium (Section 8).

- The measurement in *AA* collisions of a **thermal photon** excess over the expected prompt γ yield [42] would provide direct access to the thermodynamical properties (temperature, EoS) of the produced system (Section 9).

Among all available experimental observables, particles with large transverse momentum p_T and/or high mass ("hard probes") [43, 44] are of crucial importance for several reasons (Fig. 3): (i) they originate from partonic scatterings with large momentum transfer Q^2 and thus are directly coupled to the fundamental QCD degrees of freedom; (ii) their production time-scale is very short, $\tau \approx 1/p_T \lesssim 0.1$ fm/c, allowing them to propagate through
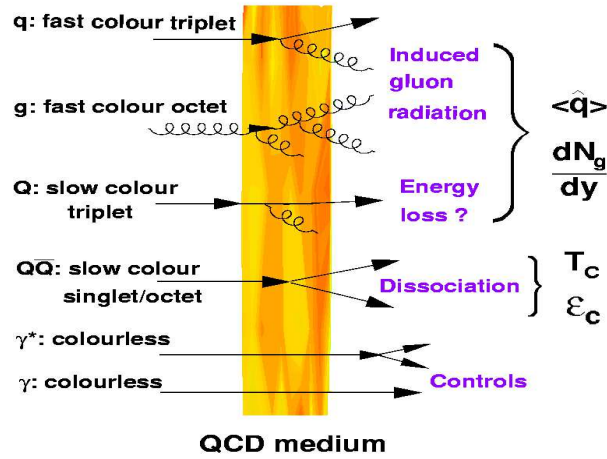
Figure 3. Examples of hard probes whose modifications in high-energy *AA* collisions provide direct information on properties of QCD matter such as the $\langle \hat{q} \rangle$ transport coefficient, the initial gluon rapidity density dN^g/dy, and the critical temperature and energy density.

(and be potentially affected by) the medium, (iii) their cross sections can be theoretically predicted using the perturbative QCD (pQCD) framework. Hard processes thus constitute experimentally- and theoretically-controlled self-generated "tomographic" probes of the hottest and densest phases of the reaction. The pQCD *factorization theorem* [45] allows one to determine the production cross section of a given hard probe as the convolution of long-distance parton distribution (PDFs, $f_{a/A}$) and fragmentation (FFs, $D_{c \to h}$) functions and the (perturbatively computable up to a given order in α_s) parton-parton scattering cross section:

$$d\sigma_{AB \to h}^{hard} = f_{a/A}(x, Q^2) \otimes f_{b/B}(x, Q^2) \otimes d\sigma_{ab \to c}^{hard} \otimes D_{c \to h}(z, Q^2) + \mathcal{O}(1/Q^2) \quad (3)$$

The validity of Eq. (3) holds on the possibility to separate long- and short-distance effects with independent QCD time (length) scales as well as on the assumption of *incoherent* parton-parton scatterings. In *AA* collisions, the incoherence condition for hard processes implies: $f_{a/A} \approx A \cdot f_{a/N}$, i.e. that, in the *absence* of medium effects, the parton flux in a nucleus A should be the same as that of a superposition of A independent nucleons. Thus,

$$d\sigma_{AB \to h}^{hard} \approx A \cdot B \cdot f_{a/p}(x, Q^2) \otimes f_{b/p}(x, Q^2) \otimes d\sigma_{ab \to c}^{hard} \otimes D_{c \to h}(z, Q^2), \quad (4)$$

and minimum-bias hard cross sections in *AB* collisions are expected to scale simply as $d\sigma_{AA}^{hard}|_{MB} = A \cdot B \cdot d\sigma_{pp}^{hard}$. In the most general case, for a given *AB* reaction with arbitrary impact parameter b the yield can be obtained by multiplying the cross sections measured in *pp* collisions with the ratio of the incident parton flux of the two nuclei: $dN_{AB}^{hard}(b) = \langle T_{AB}(b) \rangle \cdot d\sigma_{pp}^{hard}$, where $T_{AB}(b)$ (normalised to $A \cdot B$) is the nuclear overlap function at b determined within a purely geometric Glauber eikonal model using the measured Woods-Saxon distribution for the colliding nuclei [46]. The standard method to quantify the effects of the medium on the yield of a hard probe produced in a *AA* reaction is thus given by the *nuclear modification factor*:

$$R_{AA}(p_T, y; b) = \frac{d^2 N_{AA}/dy dp_T}{\langle T_{AA}(b) \rangle \times d^2 \sigma_{pp}/dy dp_T}, \quad (5)$$

which measures the deviation of *AA* at *b* from an incoherent superposition of *NN* collisions. This normalization is usually known as "binary collision scaling".

2. Experiments in high-energy heavy-ions physics

The Relativistic Heavy Ion Collider (RHIC) [47] at Brookhaven National Laboratory is a 3.8-km circumference accelerator composed of two identical, quasi-circular rings of super-conducting magnets ($\sim$400 dipoles and $\sim$500 quadrupoles) with six crossing-points. The machine, which started operation in 1999, can accelerate nuclei (protons) up to a maximum of 100 (250) GeV/c per nucleon. The center-of-mass energies in *AA* and $p(d)A$ collisions, $\sqrt{s_{NN}} = 200$ GeV ($\sqrt{s} = 500$ GeV for pp), are more than an order of magnitude larger than those at the CERN SPS ($\sqrt{s_{NN}} = 17.3$ GeV). The currently attained average *AA* luminosities§, $\langle \mathscr{L} \rangle \approx 4 \times 10^{26}$ cm^{-2}s^{-1} = 0.4 mb^{-1}s^{-1} are twice the design luminosity thanks mainly to an improved vacuum system [48]. There are four dedicated experiments at RHIC: two large multi-detector systems (PHENIX and STAR, Fig. 4) and two smaller specialised spectrometres (BRAHMS and PHOBOS).

BRAHMS [49] has two movable magnetic spectrometer arms with hadron identification (π, K, p) capabilities up to very large rapidities ($y_{max} \approx 4$ for charged pions). The two spectrometers consist of a total of 5 tracking chambers and 5 dipole magnets (maximum field of 1.7 T), plus 2 Time-Of-Flight systems and a Ring Imaging Čerenkov Detector (RICH) for particle identification. The angular coverage of the forward spectrometer (FS) goes from 2.3° $< \theta < 30$° (solid angle of 0.8 msr) up to momenta of 35 GeV/c. The midrapidity spectrometer (MSR) covers 30° $< \theta < 95$° (acceptance 6.5 msr). The PHOBOS experiment [50] is based on silicon pad detectors and covers nearly the full solid angle (11 units of pseudorapidity) for charged particles, featuring excellent global event characterization at RHIC. PHOBOS consists of 4 subsystems: a multiplicity array ("octagon", $|\eta| < 3.2$, and "rings", $|\eta| \lesssim 5.4$), a finely segmented vertex detector, a two-arm magnetic spectrometer (with dipole magnet of strength 1.5 Tm) at midrapidity including a time-of-flight wall, and several trigger detectors. Particle identification (PID) is based on time-of-flight and energy loss in the silicon.

PHENIX [51] is a high interaction-rate experiment specifically designed to measure hard QCD probes such as high-p_T hadrons, direct γ, lepton pairs, and heavy flavour. PHENIX (Fig. 4, left) achieves good mass and PID resolution, and small granularity by combining 13 detector subsystems ($\sim$350,000 channels) divided into: (i) 2 central arm spectrometers for electron, photon and hadron measurement at mid-rapidity ($|\eta| < 0.35$, $\Delta\phi = \pi$); (ii) 2 forward-backward spectrometers for muon detection ($|\eta| = 1.15$ - 2.25, $\Delta\phi = 2\pi$); and (iii) 4 global (inner) detectors for trigger and centrality selection. Two types of electromagnetic calorimeters, PbSc and PbGl, measure γ and $e^{\pm}$. Additional electron identification is possible thanks to the RICH detector. Charged hadrons are measured in the axial central magnetic field (strength

§ Note that the "equivalent-pp luminosity" for hard processes, obtained scaling by the number of nucleon-nucleon collisions, is a much larger value: $\langle \mathscr{L} \rangle_{pp-equiv} = A^2 \cdot \langle \mathscr{L} \rangle_{AA} = 15\ \mu$b^{-1}s^{-1}.
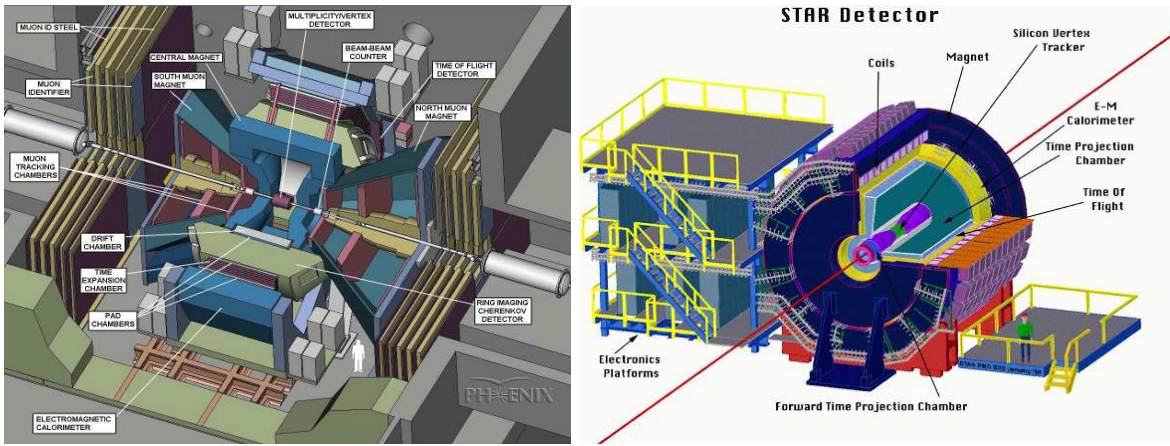
Figure 4. The two large experiments at RHIC: PHENIX [51] (left) and STAR [52] (right).

1.15 Tm) by a drift chamber (DC) and 3 layers of MWPC's with pad readout (PC). Hadron identification ($\pi^{\pm}$, $K^{\pm}$, and $p, \bar{p}$) is achieved by matching the reconstructed tracks to hits in a time-of-flight wall (TOF). Triggering is based on two Beam-Beam Counters (BBC, $|\eta| =$ 3.0 - 3.9) and the Zero Degree Calorimeters (ZDC, with $|\theta| < 2$ mrad). PHENIX features a state-of-the-art DAQ system capable of recording $\sim$300 MB/s to disk with event sizes of $\sim$100 KB (i.e. coping with event rates of $\sim$3 kHz).

The STAR experiment [52] is based around a large-acceptance Time Projection Chamber (TPC) inside a solenoidal magnet with radius 260 cm and maximum field strength 0.5 T (Fig. 4, right). The TPC with radius 200 cm and full azimuthal acceptance over $|\eta| <$1.4 provides exceptional charged particle tracking and PID via ionization energy loss dE/dx in the TPC gas and reconstruction of secondary vertices for weakly decaying particles. Additional tracking is provided by inner silicon drift detectors at midrapidity and forward radial-drift TPCs at 2.5$< |\eta| <$4. Photons and electrons are measured in the Barrel and Endcap Electromagnetic Calorimeters (EMC) covering -1.0$< \eta <$2.0 and full ϕ. The large STAR coverage allows for multi-particle correlation studies, jet reconstruction in *pp*, and also measurement of strange and charm hadrons. Triggering is done with the ZDCs, forward scintillators (Beam-Beam counters), a barrel of scintillator slats surrounding the TPC, and the EMC.

NA60 [53] is a high interaction-rate *fixed-target* experiment focused on the study of dimuon, vector meson and open charm production in *pA* and *AA* collisions at the CERN SPS. The 17 m long muon spectrometer previously used by NA38 and NA50, is composed of 8 multi-wire proportional chambers, 4 scintillator trigger hodoscopes, and a toroidal magnet. This spectrometer is separated by a $\sim$ 5 m long hadron absorber (mostly carbon) from the vertex region, where a silicon tracker made of pixel detectors [54] placed in a 2.5 T dipole field, measures the produced charged particles. The matching between the muons and the vertex tracks leads to an excellent dimuon mass resolution.

3. Benchmark channels in the vacuum and in cold QCD matter

Proton-proton collisions are the baseline free-space reference to which one compares the *AA* results in order to identify initial- or final-state effects which modify the expectation of equation (4) and can thus provide direct information on the underlying QCD medium. Figure 5 collects six different p_T-differential inclusive cross sections measured at RHIC in *pp* collisions at $\sqrt{s} = 200$ GeV: jets [55], charged hadrons [56], neutral pions [57], direct photons [58], D, B mesons (indirectly measured via $e^{\pm}$ from their semileptonic decay) [59] all at central rapidities ($y = 0$), and negative hadrons at forward rapidities ($\eta = 3.2$) [60]. The measurements cover 9 orders of magnitude in cross section (from 10 mb down to 10 pb), and broad ranges in transverse momentum (from zero momentum for D, B mesons up to $\sim$45 GeV/c, a half of the kinematical limit, for jets) and rapidity (from $\eta = 0$ up to $\eta = 3.2$ for h^- and even, not shown here, $y = 3.8$ for π°'s [61]). Whenever there is a concurrent measurement of the same observable by two or more RHIC experiments, the data are consistent with each other (the only exception being the heavy-flavour electron cross sections, which are a factor 2-3 larger in STAR [62] than in PHENIX [59]).
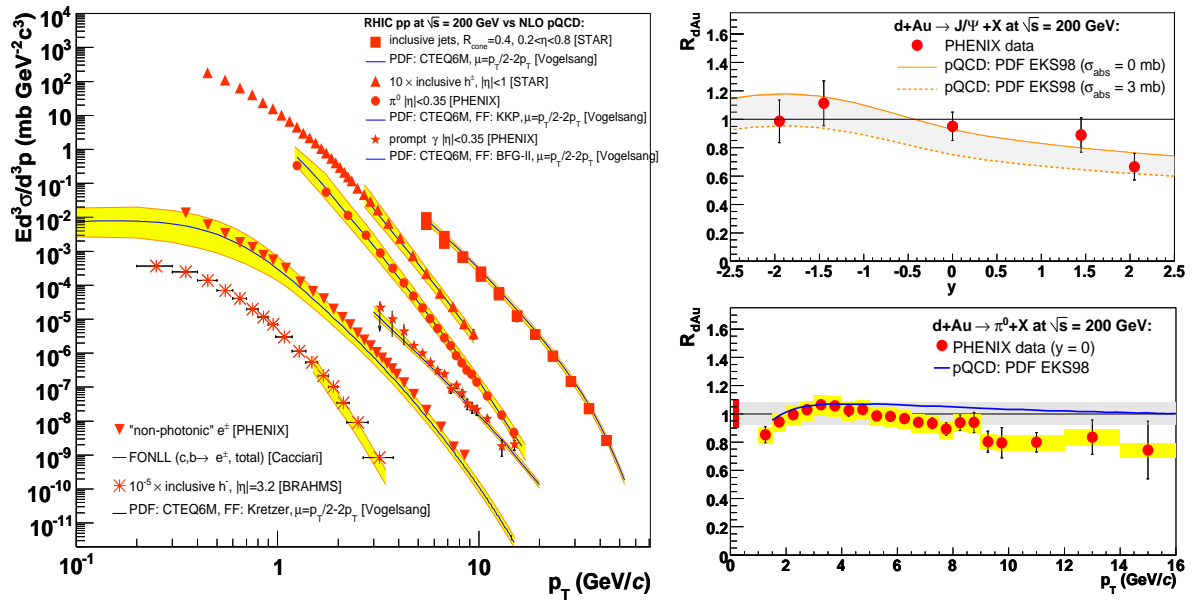

Figure 5. Left: Compilation of hard cross sections in *pp* collisions at $\sqrt{s} = 200$ GeV (10%-30% syst. uncertainties not shown for clarity purposes) measured by STAR [55, 56], PHENIX [57, 58, 59], and BRAHMS [60] compared to NLO [63, 64] and NLL [65] pQCD predictions (yellow bands). Right: Nuclear modification factors for J/ψ versus rapidity [71] (top), and for high-p_T π° at mid-rapidity [72] (bottom) in central dAu collisions at $\sqrt{s_{NN}} = 200$ GeV compared to pQCD calculations [73, 74] with EKS98 [75] nuclear shadowing.

Standard next-to-leading-order (NLO) [63, 64] or resummed next-to-leading log (NLL) [65] perturbative QCD calculations with modern proton PDFs [66], hadron fragmentation functions [67, 68], and with varying factorization-renormalization scales ($\mu = p_T/2 - 2p_T$) show an overall good agreement with the available *pp* data at $\sqrt{s} = 200$ GeV (yellow bands in Fig.

5, left). This is true even in the semi-hard range $p_T \approx 1 - 4$ GeV/c, where a perturbative description would be expected to give a poorer description of the spectra. These results indicate that the hard QCD cross sections at RHIC energies are well under control both experimentally and theoretically in their full kinematic domain. This is at variance with measurements at lower (fixed-target) energies where several data-theory discrepancies still remain [69, 70].

Not only the proton-proton hard cross sections are well under control theoretically at RHIC but the hard yields in deuteron-nucleus collisions do not show any significant deviation from the perturbative expectations. Figure 5 right, shows the nuclear modification factors measured in *dAu* collisions at $\sqrt{s_{NN}} = 200$ GeV for J/ψ, $R_{dAu}(y)$ [71], and for leading π°, $R_{dAu}(p_T)$ at $y = 0$ [72]. At *mid-rapidity*, the maximum deviation from the $R_{dAu} = 1$ expectation for hard processes without initial-state effects is of the order of $\sim$20%. Both $R_{dAu}(y, p_T)$ ratios are well accounted for by standard pQCD calculations [73, 74] that include DGLAP-based parametrizations of nuclear shadowing [75] and/or a mild amount of initial-state p_T broadening [76] to account for a modest "Cronin enhancement" [77]. These data clearly confirm that at mid rapidities, the parton flux of the incident gold nucleus can be basically obtained by geometric superposition of the nucleon PDFs, and that the nuclear (x, Q^2) modifications of the PDFs are very modest. Since no final-state dense and hot system is expected to be produced in *dAu* collisions, such results indicate that any deviations from $R_{AA} = 1$ larger than $\sim$40% potentially observed for hard probes in *AuAu* collisions (at central rapidities) can only be due to *final*-state effects in the medium produced in the latter reactions.

4. Low-x gluon saturation: *AA* rapidity densities, and high-p_T *dA* forward suppression

The bulk hadron multiplicities measured at mid-rapidity in central *AuAu* at $\sqrt{s_{NN}} = 200$ GeV $dN_{ch}/d\eta|_{\eta=0} \approx 700$, are comparatively lower than the $dN_{ch}/d\eta|_{\eta=0} \approx 1000$ expectations of "minijet" dominated scenarios [78], soft Regge models [79] (without accounting for strong shadowing effects [80]), or extrapolations from an incoherent sum of proton-proton collisions [81] (Fig. 6, left). However, Colour Glass Condensate (CGC) approaches [34, 82] which effectively take into account a reduced *initial* number of scattering centers in the nuclear PDFs, $f_{a/A}(x, Q^2) < A \cdot f_{a/N}(x, Q^2)$, agree well with experimental data. In the saturation models non-linear effects become important and start to saturate the parton densities when the area occupied by the partons becomes similar to that of the hadron, πR^2. For a nucleus with A nucleons and total gluon distribution $xG(x, Q^2)$ this condition translates into the following saturation momentum [83, 84]:

$$Q_s^2(x) \simeq \alpha_s \frac{1}{\pi R^2} xG(x, Q^2) \sim A^{1/3} x^{-\lambda} \sim A^{1/3} (\sqrt{s})^\lambda \sim A^{1/3} e^{\lambda y}, \qquad (6)$$

with $\lambda \approx 0.2$–0.3 [34]. The mass number dependence implies that, at comparable energies, non-linear effects will be $A^{1/3} \approx 6$ times larger in a heavy nucleus ($A \sim 200$ for *Au* or *Pb*) than in a proton. Based on the general expression (6), CGC-based models can describe the centrality and c.m. energy dependences of the bulk *AA* hadron production (Fig. 6, right).
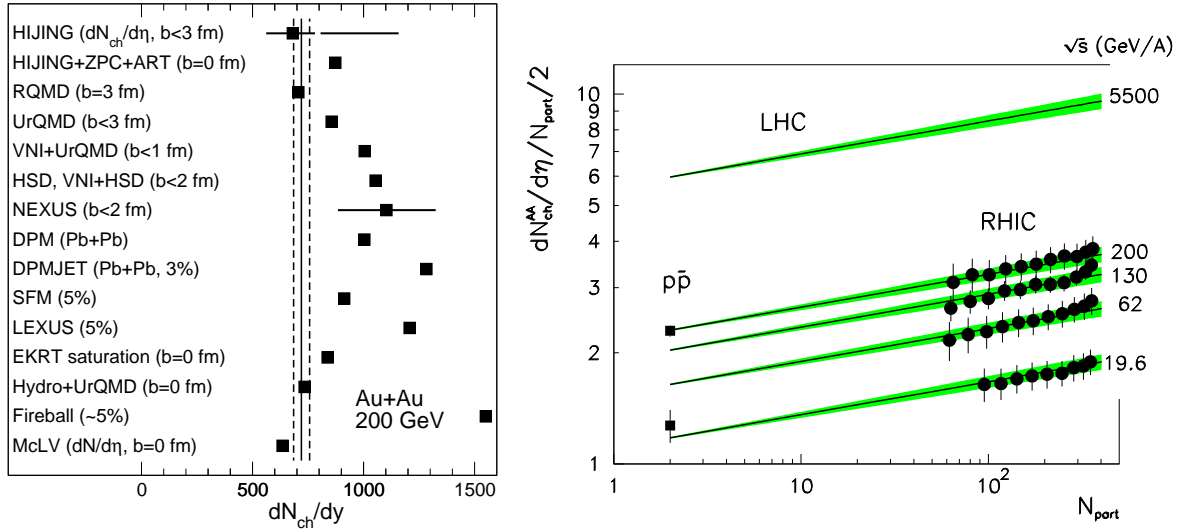
Figure 6. Left: Data vs. models for $dN_{ch}/d\eta|_{\eta=0}$ in central *AuAu* at $\sqrt{s_{NN}} = 200$ GeV [30, 81] (the saturation model prediction is identified as McLV [85]). Right: Energy- and centrality- (in terms of the number of nucleons participating in the collision, N_{part}) dependences of $dN_{ch}/d\eta|_{\eta=0}$ (normalised by N_{part}): PHOBOS data [30] versus the saturation prediction [82] .

The second manifestation of CGC-like effects in the RHIC data is the BRAHMS observation of suppressed yields of moderately high-p_T hadrons ($p_T \approx 2-4$ GeV/c) in *dAu* relative to *pp* collisions at forward rapidities ($\eta \approx 3.2$, Fig. 7) [60]. Hadron production at such small angles is theoretically sensitive to partons in the *Au* nucleus with $x_2^{min} = \left(p_T/\sqrt{s_{NN}}\right)\exp(-\eta) \approx \mathcal{O}(10^{-3})$ [74]. The observed nuclear modification factor, $R_{dAu} \approx 0.8$, cannot be reproduced by pQCD calculations that include the same *leading-twist* nuclear shadowing [74, 86, 87] that describes the *dAu* data at $y = 0$ (Fig. 5, right) but can be described by CGC approaches that parametrise the *Au* nucleus as a saturated gluon wavefunction [88, 89, 90].
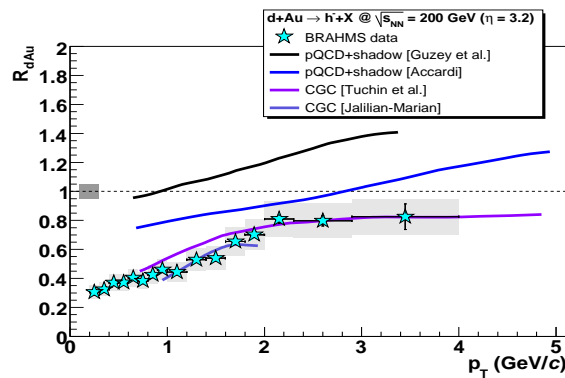

Figure 7. Nuclear modification factor $R_{dAu}(p_T)$ for negative hadrons measured at forward rapidities by BRAHMS in *dAu* at $\sqrt{s_{NN}} = 200$ GeV [60] compared to predictions of leading-twist shadowing pQCD [74, 86] (two upper curves) and CGC [88, 89] (lower curves).

It is worth noting, however, that at RHIC energies the saturation momentum is in the transition between the soft and hard regimes ($Q_s^2 \approx 2$ GeV^2) and that the results consistent with the CGC

predictions are in a kinematic range with relatively low momentum scales: $\langle p_T \rangle \sim 0.5$ GeV for the bulk hadron multiplicities and $\langle p_T \rangle \sim 2$ GeV for forward inclusive hadron production. In such a kinematic range non-perturbative effects can blur a simple interpretation based on partonic degrees of freedom alone. Following Eq. (6), the relevance of low-*x* QCD effects will certainly be enhanced at the LHC due to the increased: center-of-mass energy, nuclear radius ($A^{1/3}$), and rapidity of the produced partons [76, 91]. At the LHC, the saturation momentum $Q_s^2 \approx 5 - 10$ GeV^2 [34] will be more clearly perturbative and the relevant *x* values in *AA* and *pA* collisions will be 30–70 times lower than at RHIC: $x_2 \approx 10^{-3}(10^{-5})$ at central (forward) rapidities for processes with a hard scale $p_T \sim 10$ GeV.

5. sQGP viscosity: Strong hydrodynamical flows and AdS/CFT connection

The bulk hadron production ($p_T \lesssim 2$ GeV/*c*) in *AuAu* reactions at RHIC shows strong collective effects known as radial and elliptic flows. First, the measured single hadron p_T spectra have an inverse slope parameter T_{eff} larger than that measured in *pp* collisions, increasing with reaction centrality and with hadron mass as expected if collective expansion blue-shifts the hadron spectra. Empirically, one finds: $T_{eff} \approx T + \langle \beta_T \rangle^2 \cdot m$, with T and $\langle \beta_T \rangle$ being the freeze-out temperature and average collective flow velocity of the "fireball", and *m* the mass of the hadron. Phenomenological fits of the spectra to "blast wave" models yield transverse flow velocities $\langle \beta_T \rangle \approx 0.6$ [28]. Full hydrodynamical calculations which start with a partonic phase very shortly after impact ($\tau_0 < 1$ fm/*c*) develop the amount of collective radial flow needed to accurately reproduce all the measured hadron spectra (Fig. 8).
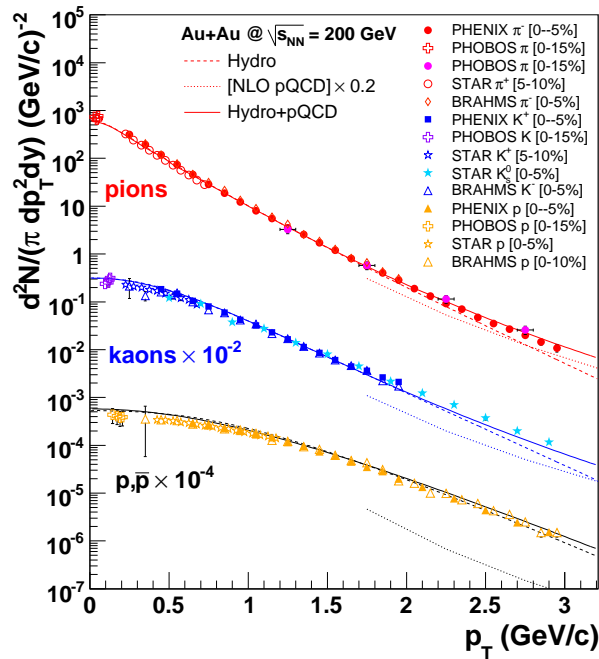

Figure 8. Transverse momentum spectra for pions, kaons, and (anti)protons measured at RHIC below $p_T \approx 3$ GeV/*c* in 0-10% central *AuAu* collisions at $\sqrt{s_{NN}} = 200$ GeV compared to hydrodynamics(+pQCD) calculations [92].
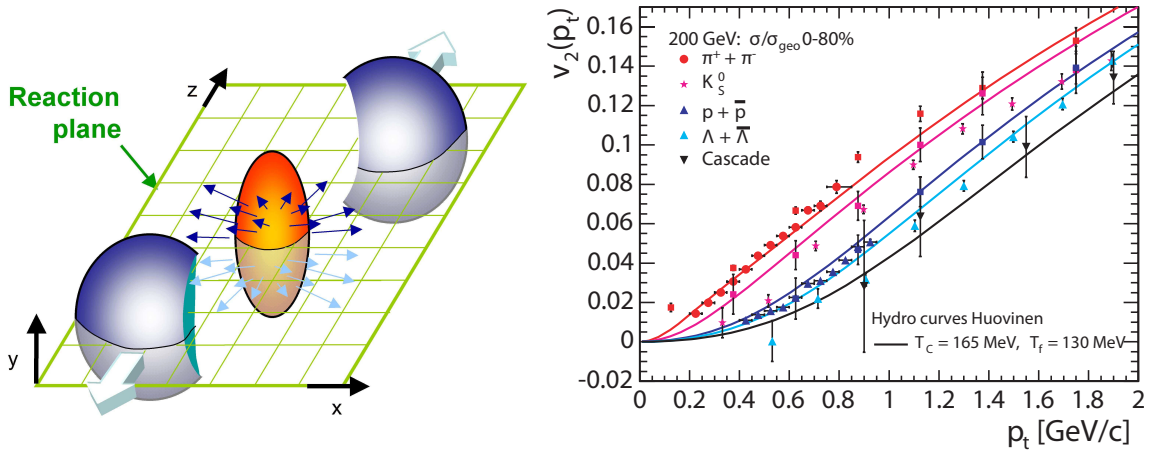
Figure 9. Left: Spatial asymmetry with respect to the reaction plane of the produced "fireball" in non-central nucleus-nucleus collisions. Right: Measured elliptic flow parameter $v_2(p_T)$ below $p_T = 2\,\text{GeV}/c$ for a variety of hadrons [97] compared to hydrodynamic predictions [40].

Secondly, the azimuthal distributions $dN/d\Delta\phi$ of hadrons emitted relative to the reaction plane ($\Delta\phi = \phi - \Phi_{RP}$) show a strong harmonic modulation with a preferential "in-plane" emission in non-central collisions. Such an azimuthal flow pattern is a truly collective effect (absent in pp collisions) consistent with an efficient translation of the initial coordinate-space anisotropy in AA reactions with non-zero impact parameter (i.e. with a lens-shaped overlap zone, see Fig. 9 left) into a final "elliptical" asymmetry in momentum-space. Rescattering between the produced particles drives collective motion along the pressure gradient, which is larger for directions parallel to the smallest dimension of the lens. The strength of this asymmetry is quantified via the second Fourier coefficient $v_2(p_T, y) \equiv \langle cos(2\Delta\phi) \rangle$ of the azimuthal decomposition of single inclusive hadron spectra with respect to the reaction plane [93, 94]

$$E\frac{d^3N}{d^3p} = \frac{1}{2\pi}\frac{d^2N}{p_T\,dp_T\,dy}\left(1 + 2\sum_{n=1}^{\infty} v_n\,cos[n(\phi - \Phi_{RP})]\right). \qquad (7)$$

The large $v_2 \approx 0.16$ measured in the data (Fig. 9, right) indicates a strong degree of collectivity (pressure gradients) building up in the first instants of the collision. Indeed, elliptic flow develops in the initial phase of the reaction and quickly self-quenches beyond $\tau \approx 5\,\text{fm}/c$ as the original spatial eccentricity disappears [95]. Two additional experimental observations support the existence of an efficient hydrodynamical response with very short thermalization times. First, not only light hadrons but also D, B mesons (indirectly measured via their semileptonic decays into $e^{\pm}$) show momentum anisotropies with v_2 as large as 10% [96]. The fact that the heavy c and b quarks participate in the common flow of the medium is clearly suggestive of a robust collective response during the early *partonic* phase. In addition, the v_2 values measured for different centralities, at different center-of-mass energies (200 and 62 GeV) and for different colliding systems (*AuAu* and *CuCu*) are found to show simple scaling laws with the reaction eccentricity [98, 99] also in agreement with hydrodynamics expectations.
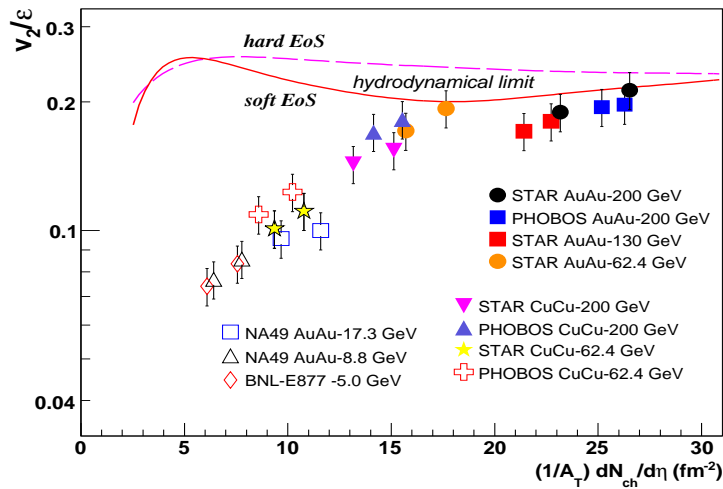
Figure 10. Elliptic flow (normalised by the participant eccentricity [98]) v_2/ε as a function of the hadron rapidity density $dN_{ch}/d\eta|_{\eta=0}$ normalised by the reaction overlap area $A_\perp$, measured at SPS [104] and RHIC [98, 105] compared to the "hydrodynamical limit" expectations for a fully thermalised system with hard (HRG-like) or soft (QGP-like) EoS [95, 102, 108]. Adapted from [105, 98] (10% errors have been added to approx. account for v_2, ε syst. uncertainties).

These results have attracted much attention for several reasons. First, the strong v_2 seen in the data is not consistent with the much lower values, $v_2 \lesssim 6\%$, expected by transport models of hadronic matter [100] or for a partonic system rescattering with perturbative cross sections ($\sigma_{gg} \approx 3$ mb) [101]. The magnitude, and the p_T and hadron mass dependences of the radial and elliptic flows below $p_T \approx 2$ GeV/c are, however, well described by *ideal* hydrodynamics models whose space-time evolution starts with a realistic QGP Equation of State (EoS) with initial energy densities $\varepsilon_0 \approx 30$ GeV/fm^3 at thermalization times $\tau_0 \approx 0.6$ fm/c [22, 40, 102, 103] (Fig. 9). Second, such a degree of accord between relativistic hydrodynamics and the data was absent at lower CERN-SPS energies [104]. Fig. 10 shows the particle-density dependence of the v_2 parameter (scaled by the eccentricity of the reaction ε to remove centrality-dependent geometrical effects) measured in semicentral collisions at different c.m. energies. The fact that SPS data lie below the "hydrodynamical limit" curves [108, 95] estimated for a system completely thermalised, suggests that equilibration is only partially achieved at the top SPS energy [104]. RHIC v_2 data in the range $\sqrt{s_{NN}} \approx 62$ – 200 GeV [105, 106, 98] are, however, close to the full thermalization expectations. Third, inclusion of viscous (i.e. "internal dissipation") corrections to the ideal fluid dynamics equations spoils the reproduction of $v_2(p_T)$, especially above $p_T \approx 1$ GeV/c where even a modest viscosity brings v_2 towards zero [109]. Estimates of the maximum amount of viscosity allowed by the $v_2(p_T)$ data [110] give a value for the dimensionless viscosity/entropy ratio close to the conjectured universal lower bound, $\eta/s = \hbar/(4\pi)$, obtained from AdS/CFT calculations [14]. Similarly, approaches [111, 112] that describe simultaneously the large $v_2(p_T)$ and quenching factors $R_{AA}(p_T)$ of heavy-flavour $e^\pm$ require small heavy-quark diffusion coefficients ($3 < 2\pi T D < 6$) which correspond to very small shear viscosities, $1 < 4\pi(\eta/s) < 2$, and/or very short thermalization times.

The fast (local) thermalization times supported by the robust collective flow generated in the first instants of the reaction, and the good agreement of the p_T- and mass-differential spectra and v_2 with *ideal* relativistic hydrodynamics models which assume a fluid evolution with zero viscosity (i.e. with negligible internal shear stress), have been presented as evidences that the matter formed at RHIC is a *strongly interacting* QGP (sQGP) [113, 114, 115, 116, 117]. This new state of matter – with *liquid*-like properties e.g. a Coulomb coupling parameter $\Gamma = \langle E_{pot} \rangle / \langle E_{kin} \rangle \sim g^2 (4^{1/3} T) / (3T) \sim 3$ for $g^2 \sim 4 - 6$ at $T \approx 200$ MeV [118, 116] – challenges the anticipated paradigm [2] of a weakly interacting gas of relativistic partons (with $\Gamma \ll 1$), lending support to the application of strongly-coupled-gauge/weakly-coupled-gravity duality techniques [14, 15, 16] to compute relevant sQGP parameters.

It is worth noting, however, that recent lattice results predict a QCD transition temperature, $T_{crit} \approx 190$ MeV [119], which is $\sim$30–40 MeV larger than the freeze-out temperature extracted from observed particle yields in heavy ion experiments (dotted-dashed curve in Fig. 1) [5, 25]. Thus, an intermediate regime between the QCD transition and freeze-out could exist during which the system created in heavy ion collisions persists in a very dense strongly-interacting hadronic phase. At LHC energies the contribution from the QGP phase to the collective particle flow(s) will be much larger than at RHIC or SPS and, therefore, the v_2 will be less dependent on the details of the subsequent hadronic phase. The measurement of the differential elliptic flow properties in *AA* collisions at the LHC will be of primary importance to confirm or not the sQGP interpretation as well as to search for a possible weakening of the v_2 indicative of the existence of a weakly interacting QGP phase at higher temperatures than those of the liquid-like state found at RHIC [118, 110].

6. Parton number density and $\langle \hat{q} \rangle$ transport coefficient: High-p_T hadron suppression

Among the most exciting results of the RHIC physics programme is the observed strong suppression of high-p_T leading hadron spectra in central *AA* [120] consistent with the predicted attenuation of the parent quark and gluon jets in a dense QCD medium ("jet quenching") [121, 122]. Above $p_T \approx 5$ GeV/c, neutral mesons (π°, η) [123] and inclusive charged hadrons [56] all show a common factor of $\sim$5 suppression compared to an incoherent superposition of *pp* collisions (Fig. 11, left). Such a significant suppression was not observed at SPS where, after reevaluating the *pp* baseline spectrum [124, 125], the central-*AA* meson spectra show a R_{AA} around unity (Fig. 12, right) probably due to the cancellation of a $\sim$50% final-state suppression by initial-state Cronin broadening [124, 126, 127]. At RHIC, the $R_{AA} \approx 1$ perturbative expectation which holds for other hard probes such as "colour blind" photons [128] – and for high-p_T hadrons in *dAu* reactions (Fig. 5, right) – is badly broken ($R_{AA} \approx 0.2$) in central *AuAu* collisions. This strongly supports the picture of partonic energy loss in *final-state* interactions within the dense matter produced in the reaction.

The dominant contribution to the energy loss is believed to be of non-Abelian radiative nature
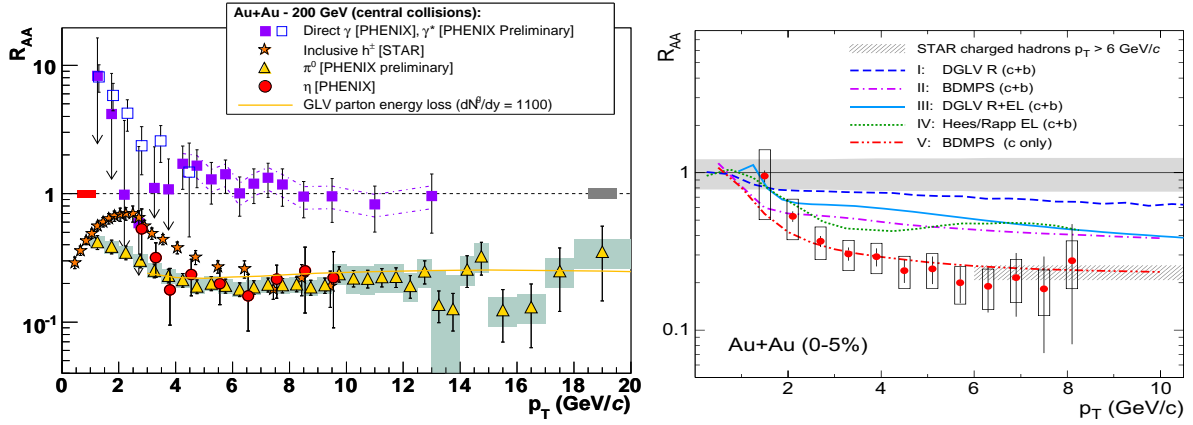
Figure 11. Nuclear modification factor $R_{AA}(p_T)$ for γ, π°, η [123], $\gamma^\star$ [96], and $h^\pm$ [56] (left) and for "non-photonic" $e^\pm$ from D,B mesons [62] (right) in central *AuAu* at $\sqrt{s_{NN}} = 200$ GeV compared to various parton energy loss model predictions [130, 133, 136, 112].

(i.e. due to gluon radiation) as described in the GLV [129, 130] and BDMPS [35, 131] (or LPCI [132]) formalisms. In the GLV approach, the initial gluon density dN^g/dy of the expanding plasma (with transverse area $A_\perp$ and length L) can be estimated from the measured energy loss ΔE:

$$\Delta E \propto \alpha_S^3 C_R \frac{1}{A_\perp} \frac{dN^g}{dy} L \,. \tag{8}$$

where C_R is the Casimir colour factor of the parton (4/3 for quarks, 3 for gluons). In the BDMPS framework, the transport coefficient‖ $\langle \hat{q} \rangle$, characterizing the squared average momentum transfer of the hard parton per unit distance, can be derived from the average energy loss according to:

$$\langle \Delta E \rangle \propto \alpha_S C_R \langle \hat{q} \rangle L^2 . \tag{9}$$

From the general Eqs. (8) and (9), very large initial gluon rapidity densities, $dN^g/dy \approx 1100 \pm 300$ [130], or equivalently, transport coefficients $\langle \hat{q} \rangle \approx 11 \pm 3$ GeV^2/fm [134, 135, 136, 137], are required in order to explain the observed amount of hadron suppression at RHIC. The corresponding values for SPS are $dN^g/dy \approx 400 \pm 100$ and $\langle \hat{q} \rangle \approx 3.5 \pm 1$ GeV^2/fm [138].

Most of the empirical properties of the quenching factor for light-flavour hadrons – magnitude, p_T-, centrality-, $\sqrt{s_{NN}}$- dependences of the suppression – are in quantitative agreement with the predictions of non-Abelian parton energy loss models (Fig. 12). However, the fact that the high-p_T $e^\pm$ from semi-leptonic D and B decays is as suppressed as the light hadrons in central *AuAu* (Fig. 11, right) [139, 62] is in apparent conflict with the robust $\Delta E_{\text{heavy}-Q} < \Delta E_{\text{light}-q} < \Delta E_g$ prediction of radiative energy loss models. Since the gluonsstrahlung probability of quarks and gluons is completely determined by the gauge structure (Casimir factors) of SU(3), the colour octet gluons (which fragment predominantly into *light* hadrons)

‖ Technically, the $\hat{q}$ parameter can be identified with the coefficient in the exponential of an adjoint Wilson loop averaged over the medium length: $\langle W^A(C) \rangle \equiv exp\left[(-1/4\sqrt{2})\hat{q}L^-L^2\right]$ [15].
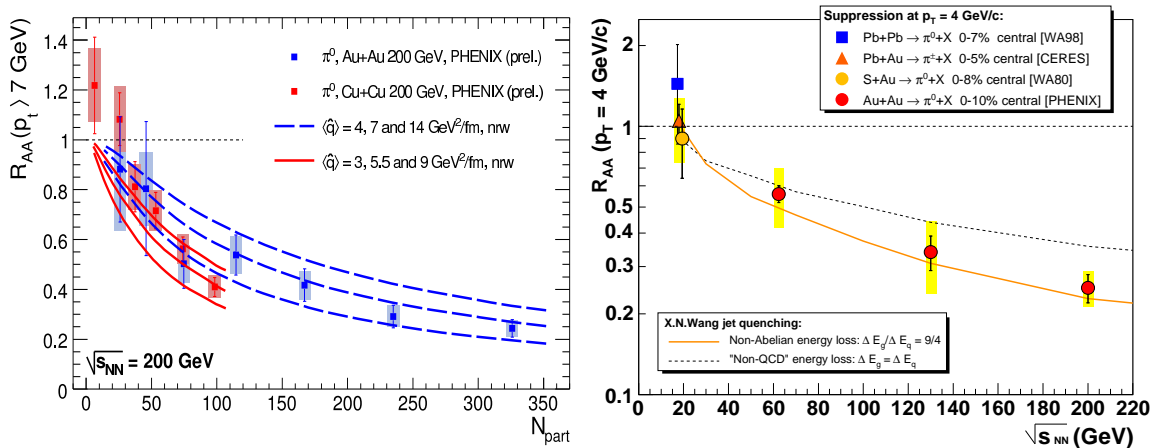
Figure 12. Left: Centrality dependence of $R_{AA}(p_T > 7$ GeV/$c)$ for π° in *AuAu* and *CuCu* collisions at $\sqrt{s_{NN}} = 200$ GeV compared to the BDMPS-based PQM model [134, 137] for different values of the $\langle \hat{q} \rangle$ coefficient. Right: Excitation function of the nuclear modification factor, $R_{AA}(\sqrt{s_{NN}})$, for π° in central *AA* reactions at a fixed $p_T = 4$ GeV/c [138], compared to predictions of a jet-quenching model with canonical non-Abelian (solid line) energy loss [141].

are expected to lose energy at $C_A/C_F = 9/4$ times the rate of quarks. In addition, massive c, b quarks are expected to lose less energy than light ones due to their suppressed small-angle gluon radiation already in the vacuum ("dead-cone" effect) [140]. In order to reproduce the high-p_T open charm/bottom suppression, jet quenching models require either initial gluon rapidity densities ($dN^g/dy \approx 3000$) [133] inconsistent with the total hadron multiplicities, $dN^g/dy \approx 1.8 dN_{ch}/d\eta|_{\eta=0}$ [138] or with the dN^g/dy needed to describe the quenched light hadron spectra, or they need a smaller relative contribution of B relative to D mesons than theoretically expected in the measured decay electron p_T range [136]. This discrepancy¶ may point to an additional contribution from elastic (i.e. non-radiative) energy loss [142, 143] for heavy-quarks [133] which was considered negligible so far [122]. The unique possibility at the LHC to fully reconstruct jets [144], to tag them with prompt γ [145] or Z [146] and to carry out detailed studies in the c, b quark sector [147, 148] will be very valuable to clarify the response of strongly interacting matter to fast heavy-quarks, and will provide accurate information on the transport properties of QCD matter [15, 16].

7. Propagation of collective perturbations in QCD matter: Distorted di-jet correlations

Full jet reconstruction in *AA* collisions with standard jet algorithms [149] is unpractical at RHIC energies due to low cross-sections for high-E_T jets and the overwhelming background of soft particles in the underlying event (only above ∼30 GeV are jets above the background). Instead, jet-like correlations at RHIC are conventionally measured on a statistical basis by selecting high-p_T *trigger* particles and measuring the azimuthal ($\Delta\phi = \phi - \phi_{trig}$) and rapidity

¶ Note, however, that the theoretical and experimental control of the $pp \to D, B + X$ reference (Fig. 5, left) is not as good as for the light hadron spectra [136].

($\Delta\eta = \eta - \eta_{trig}$) distributions of *associated* hadrons ($p_{T,assoc} < p_{T,trig}$) relative to the trigger:

$$C(\Delta\phi, \Delta\eta) = \frac{1}{N_{trig}} \frac{d^2 N_{pair}}{d\Delta\phi d\Delta\eta}. \tag{10}$$

Combinatorial background contributions, corrections for finite pair acceptance, and the superimposed effects of global azimuthal modulations (elliptic flow) are taken into account with different techniques [150, 151, 152, 153]. In *pp* or *dAu* collisions, a dijet signal appears as two distinct back-to-back Gaussian-like peaks around $\Delta\phi = 0$ (near-side) and $\Delta\phi = \pi$ (away-side) (*dAu* panel in Fig. 13). At variance with this standard dijet topology in the QCD vacuum, early STAR results for semihard jets in central *AuAu* reactions [150] showed a complete disappearance of the opposite side peak for $3 < p_{T,assoc} < 4 < p_{T,trig} < 6$ GeV/c while the near-side correlation remained unchanged (Fig. 13, leftmost panel). Such a monojet-like topology confirmed a jet-quenching picture where a $2 \to 2$ hard scattering takes place near the surface of the system with the trigger parton being unaffected and the away-side parton losing energy while traversing a medium opaque to coloured probes. For rising $p_{T,trig}$, the away-side parton is seen to increasingly "punchthrough" the medium [150], although the azimuthally-opposite correlation strength is still significantly reduced compared to *dAu* (Fig. 13).
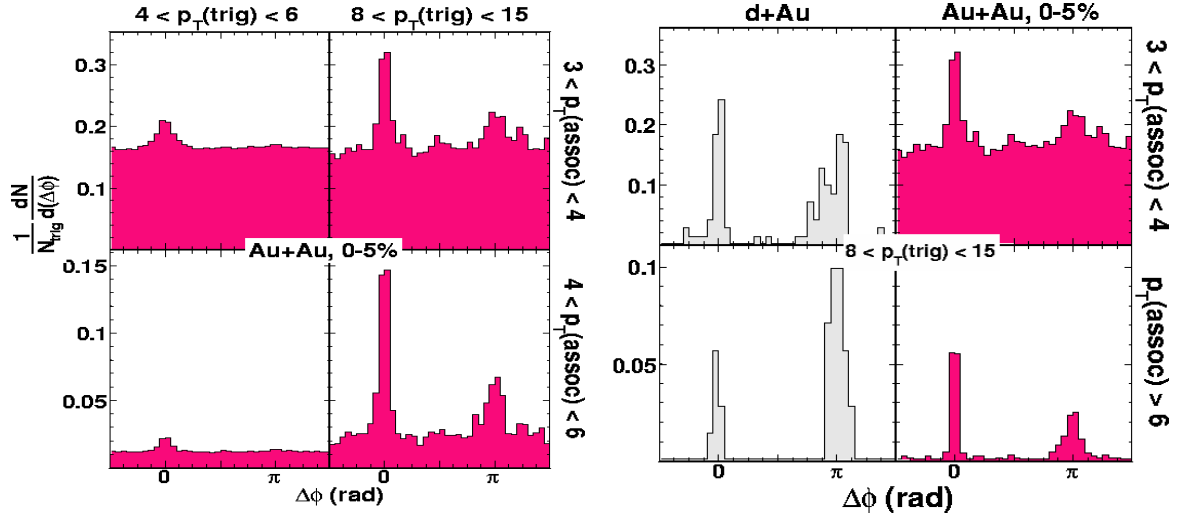

Figure 13. Angular correlations of high-p_T charged hadron pairs measured in: 0-5% central *AuAu* events in various $p_{T,trig}$ and $p_{T,assoc}$ (GeV/c) ranges (left), and in *dAu* and 0-5%-central *AuAu* for fixed $p_{T,trig} = 8 - 15$ GeV/c and two $p_{T,assoc}$ ranges [154] (right).

The estimated energy loss, Eqs. (8) and (9), of the quenched partons is very large, up to $\Delta E_{loss} \approx 3$ GeV/fm for a 10 GeV parton [137] and most of the (mini)jets, apart from those close to the surface, dump a significant fraction of their energy and momentum in a cell of about 1 fm^3 in the rest frame of the medium. Since energy and momentum are conserved, the fragments of the quenched parton are either shifted to lower energy ($p_T < 2$ GeV/c) and/or scattered into a broadened angular distribution. Both softening and broadening of the away-side distribution are seen in the data [151] when the p_T threshold of the away-side associated hadrons is *lowered*. Fig. 14 shows the dihadron azimuthal correlations $dN_{pair}/d\Delta\phi$ in central
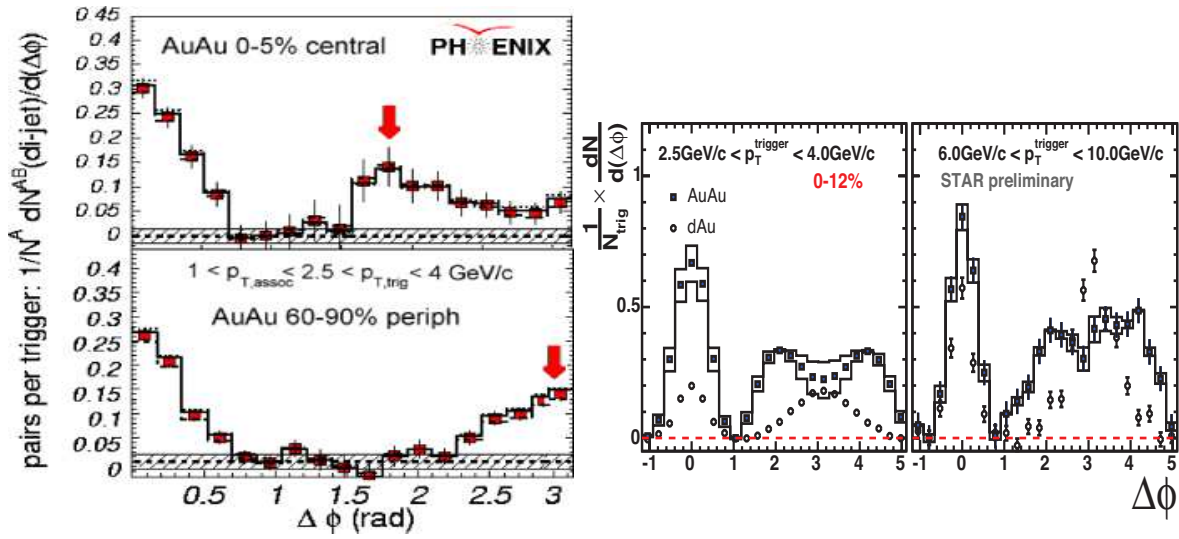
Figure 14. Azimuthal distributions of semihard hadrons ($p_{T,assoc} = 1 - 2.5$ GeV/c) relative to a higher p_T trigger hadron measured at RHIC. Left: PHENIX data in central (top) and peripheral (bottom) *AuAu* [152] (the arrows indicate the local maxima in the away-side hemisphere). Right: STAR data in central *AuAu* (squares) and *dAu* (circles) for two ranges of $p_{T,trig}$ [155].

AuAu collisions for $p_{T,assoc} = 1 - 2.5$ GeV/c [152, 155]. In this semi-hard range, the away-side hemisphere shows a very unconventional angular distribution with a "dip" at $\Delta\phi \approx \pi$ and two neighbouring local maxima at $\Delta\phi \approx \pi \pm 1.1$. Such a non-Gaussian "volcano"-like profile has been explained as due to the preferential emission of energy from the quenched parton at a finite angle with respect to the jet axis. This could happen in a purely radiative energy loss scenario [156] but more intriguing explanations for the conical-like pattern have been put forward based on the dissipation of the lost energy into a collective mode of the medium which generates a wake of lower energy gluons with Mach- [157, 158, 159] or Čerenkov-like [159, 160, 161] angular emissions. In the Mach-cone scenario, the *speed of sound*[+] of the traversed matter, $c_s^2 = \partial P/\partial\varepsilon$, can be determined from the characteristic supersonic angle of the emitted secondaries: $\cos(\theta_M) = \langle c_s \rangle$, where θ_M is the Mach shock wave angle and $\langle c_s \rangle$ the time-averaged value of the speed of sound of the medium traversed by the parton. The resulting preferential emission of secondary partons from the plasma at a *fixed* angle $\theta_M \approx 1.1$, yields a value $\langle c_s \rangle \approx 0.45$ which is larger than that of a hadron-resonance gas ($c_s \approx 0.35$) [162], and not far from that of a deconfined QGP[*] ($c_s = 1/\sqrt{3}$). Experimental confirmation of the Mach-cone picture or other alternative emission mechanisms for the associated particles in the quenched jet requires more detailed differential studies [163] such as the ongoing analysis of three- and many-particle azimuthal correlations [164, 165].

[+] The speed of sound is a simple proportionality constant relating the fluid pressure and energy density: $P = c_s^2 \varepsilon$.
[*] Note that although lattice calculations indicate that there are $\sim 30\%$ deviations from the ideal-gas limit in the $s(T), P(T)$ and $\varepsilon(T)$ dependences up to very high T's [1], the ideal-gas relation $\varepsilon \approx 3P$ (as well as other ratios of thermodynamical potentials) approximately holds above $\sim 2T_{crit}$.

8. Bulk hadronization: Enhanced baryon yields/flows at intermediate p_T

The increasingly suppressed production of mesons above $p_T \approx 2$ GeV/c in central *AuAu* reactions at RHIC contrasts with the simultaneous *unsuppressed* $p, \bar{p}$ [166, 167, 168] and $\Lambda, \bar{\Lambda}$ [169] yields in the range $p_T \approx 2 - 4$ GeV/c. The intermediate-p_T range in *AuAu* reactions features an anomalous baryon/meson ~ 0.8 ratio which is roughly four times higher than in more elementary pp or $e^+ e^-$ interactions (Fig. 15, left). Semihard (anti)protons show an enhancement with respect to the "x_T scaling" expectation for the ratio of perturbative cross sections at different c.m. energies [170], whereas x_T scaling holds for *all* hadrons (mesons) measured in pp (*AuAu*) collisions at RHIC [167, 170, 171]. Only above $p_T \approx 6$ GeV/c [168] (Fig. 15, left) the meson/baryon ratio is again consistent with the expected yields obtained from universal fragmentation functions. Not only their spectra are enhanced, but at $p_T = 2$ GeV/c the v_2 elliptic flow parameter of baryons exceeds that of mesons ($v_2^{meson} \approx 0.16$, see Fig. 9, right) and keeps increasing up to $p_T \sim 4$ GeV/c when it finally saturates at $v_2^{baryons} \approx 0.22$ [172, 173]. All those observations clearly indicate that standard hadron production via (mini)jet fragmentation is not sufficient to explain the RHIC data for baryons at transverse momenta of a few GeV/c.
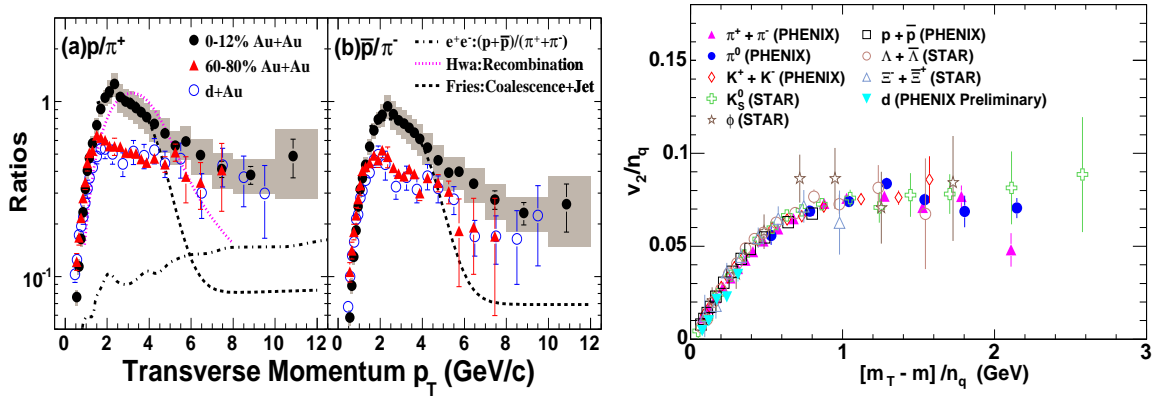

Figure 15. Left: Proton/pion in *dAu* and *AuAu* collisions at $\sqrt{s_{NN}} = 200$ GeV [168] compared to the ratio in light quark fragmentation in $e^+ e^-$ at $\sqrt{s} = 91.2$ GeV (dotted-dashed line) and to parton coalescence predictions [41]. Right: Elliptic flow parameter v_2 for all hadrons at RHIC normalised by the number of constituent quarks of each species ($n_q = 2,3$ for mesons, baryons) *vs* the transverse kinetic energy $KE_T = m_T - m$ normalised also by n_q [99, 174].

The observed baryon nuclear modification factors close to unity, the high baryon/meson ratios, and their large elliptic flow have lent support to the existence of an extra mechanism of baryon production in *AuAu* based on quark coalescence in a dense partonic medium [41]. Recombination models compute the spectrum of hadrons as a convolution of Wigner functions with single parton thermal distributions leading to an exponential distribution which dominates over the standard power-law fragmentation regime below $p_T \sim 6$ GeV/c. Coalescence models can thus reproduce the enhanced baryon production and predict also that the elliptic flow of any hadron species should follow the underlying partonic flow scaled by the number n of (recombined) constituent quarks in the hadron: $v_2(p_T) = n v_2^q(p_T/n)$,

$n = 2, 3$ for mesons and baryons, respectively [175]. Such a quark-scaling law for the elliptic flow is confirmed by the data [172, 173]. Figure 15 right, shows a recent variation of the quark-number scaling law for v_2 that uses the transverse kinetic energy ($KE_T = m_T - m$, $m_T = (p_T^2 + m^2)^{1/2}$) rather than the p_T and seems to account perfectly for the scaled v_2 of all measured species also in the soft hydrodynamical regime below $p_T \sim 2$ GeV/c [99, 174]. The overall success of valence quark coalescence models to explain hadron production in the semi-hard regime highlights the role of *thermalised* degrees of freedom in the produced system with *partonic* (as opposed to hadronic) quantum numbers.

9. Temperature and equation-of-state (EoS): Thermal photons

In order to describe the transient systems produced in *AA* collisions in terms of *thermodynamical* variables (T, ε, s, etc.) linked by an EoS which can be compared to lattice QCD expectations, it is a prerequisite to establish that the underlying degrees of freedom form, at some stage of the reaction, a statistical ensemble. Proving that *local*♯ thermalization has been attained in the course of the collision is thus a crucial issue both experimentally and theoretically [176]. The large elliptic flow signal observed in the data strongly supports the idea of fast thermalization as discussed in Section 5. The identification of real and/or virtual γ radiation from the produced "fireball" with properties consistent with a thermal distribution would in addition allow us to determine the underlying temperature and EoS of the system. Hydrodynamical [40] and parton transport [177] calculations indicate that the same cascade of secondary parton-parton collisions that drives the system towards equilibration in the first tenths of fm/c results in an identifiable emission of thermal radiation above the prompt perturbative yield in *AA* reactions in a window $p_T \approx 1 - 3$ GeV/c.
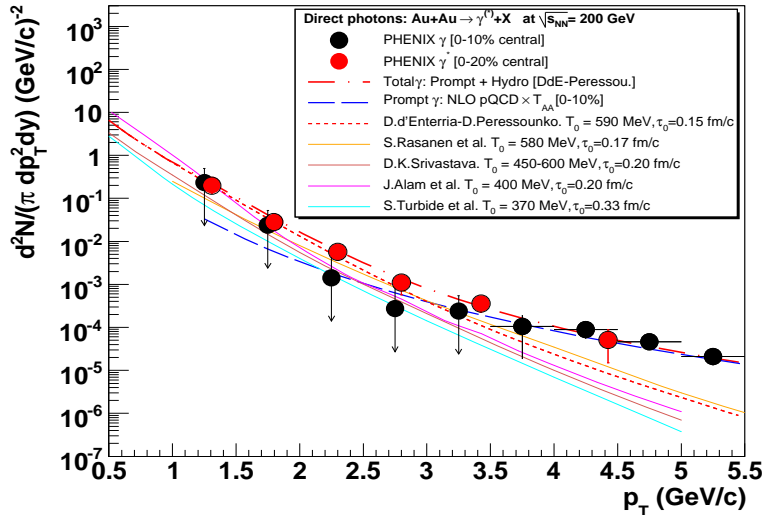

Figure 16. Direct $\gamma, \gamma^\star$ spectra measured by PHENIX [128, 96] in central *AuAu* collisions at $\sqrt{s_{NN}} = 200$ GeV compared to NLO pQCD [64] and different hydrodynamics predictions [92] including a QGP phase with $T_0 = 350\text{-}600$ MeV.

♯ Note that, by simple causality arguments, *global* equilibrium in a finite system with radius $R_A \approx 7$ fm can only occur for time-scales $\tau \gtrsim 7$ fm/c.

The preliminary γ spectrum measured in central *AuAu* by PHENIX [96, 178] is consistent with the sum of such perturbative (prompt) plus thermal (secondary) contributions (Fig. 16). Different hydrodynamical calculations of thermal photon production [92, 179, 180, 181, 182] can reproduce the PHENIX data assuming the formation of a radiating QGP with temperatures around $2T_{crit}$ ($T_0 = 400 - 600$ MeV, corresponding to average temperatures $\langle T_0 \rangle \approx 350$ MeV over the source profile) at times $\tau_0 = 2R_A/\gamma \approx 0.2$ fm/c right after the two colliding nuclei pass-through each other. A word of caution should be noted in that the baseline (T_{AA}-scaled) prompt γ spectrum at $p_T = 1 - 4$ GeV/c is obtained from NLO calculations, because no measurement is yet available in this p_T range. The confirmation of the existence of a thermal enhancement over the prompt component, will require a direct measurement of the *pp* photon spectrum down to $p_T = 1$ GeV/c.

After subtracting the prompt γ component from the inclusive direct photon spectrum, the local inverse slope parameter T_{eff} in the range $p_T \approx 2 - 4$ GeV/c can be used as a relatively good surrogate of the initial medium temperature [92]. The combination of T_{eff} with another global observable directly related to the entropy density s would therefore allow one to determine the effective number of degrees of freedom g of the system via the Stefan-Boltzmann ratio $g \propto s/T^3$. Since the final charged particle rapidity density $dN_{ch}/d\eta|_{\eta=0}$ is directly correlated with the initial entropy density of the system, by empirically studying the evolution of $g_{eff} \propto dN_{ch}/d\eta|_{\eta=0}/T_{eff}^3$ versus T_{eff} in different *AA* centralities one can effectively study the evolution of the number of degrees of freedom and look for any threshold behaviour related to the sudden increase at the transition temperature and/or a flattening of g_{eff} for temperatures above T_{crit}. Such an approach has been tested in the context of a 2D+1 hydrodynamical model which effectively reproduces the hadron and photon data at RHIC [92]. We found that one can clearly distinguish between the equation of state of a weakly interacting QGP and that of a system with hadron-resonance-gas-like EoS (i.e. with rapidly rising number of mass states with T). However, direct evidence of the parton-hadron phase change itself as a jump in g_{eff} around $T_{eff} \sim T_{crit}$ can only be potentially visible in *AuAu* reactions at *lower* center-of-mass energies ($\sqrt{s_{NN}} \approx 20 - 65$ GeV) [183]. At the LHC, the expected temperatures $\mathcal{O}(1$ GeV) reached in central *PbPb* will also produce a significant thermal photon signal up to $p_T \approx 6$ GeV/c [184] which can be used to determine the thermodynamical conditions in the *plateau* regime of the s/T^3 EoS, closer to the ideal-gas limit than at RHIC.

10. Critical temperature and energy density: Anomalous J/ψ suppression

The study of heavy-quark bound states in high-energy *AA* collisions has been long since proposed as a sensitive probe of the thermodynamical properties of the produced medium [37]. Analysis of quarkonia correlators and potentials in finite-T lattice QCD indicate that the different charmonium and bottomonium states dissociate at temperatures for which the colour (Debye) screening radius of the medium falls below their corresponding $Q\bar{Q}$ binding radius. Recent lattice analyses of the quarkonia spectral functions [185] indicate that the ground states (J/ψ and Υ) survive at least up to $T \approx 2T_{crit}$ whereas the less bounded χ_c and ψ' melt near T_{crit}.

Experimental confirmation of such a threshold-like dissociation pattern would provide a direct means to determine the transition temperature reached in the system and their comparison to *ab initio* lattice QCD predictions. A significant amount of experimental data on J/ψ production in different $p(d)A$ and AA collisions has been collected at SPS [186, 187, 188] and RHIC [189]. The corresponding nuclear modification factors compiled in [190] are shown in Fig. 17 as a function of N_{part}. The surprisingly similar amount of J/ψ suppression observed at SPS and RHIC energies (with expected temperature differences of a factor of $\sim$2) has been interpreted in a sequential-dissociation scenario [191] where the J/ψ survives up to $T \approx 2T_{crit}$ in agreement with the lattice predictions, and the observed suppression at both c.m. energies is just due to the absence of (30% and 10%) feed-down decay contributions from $\chi(1P)$ and $\psi'(2S)$ resonances which melt already at $T \approx T_{crit}$. The confirmation of such an interpretation would set an upper limit of $T \lesssim 2T_{crit} \approx 400$ MeV for the temperatures reached at RHIC.
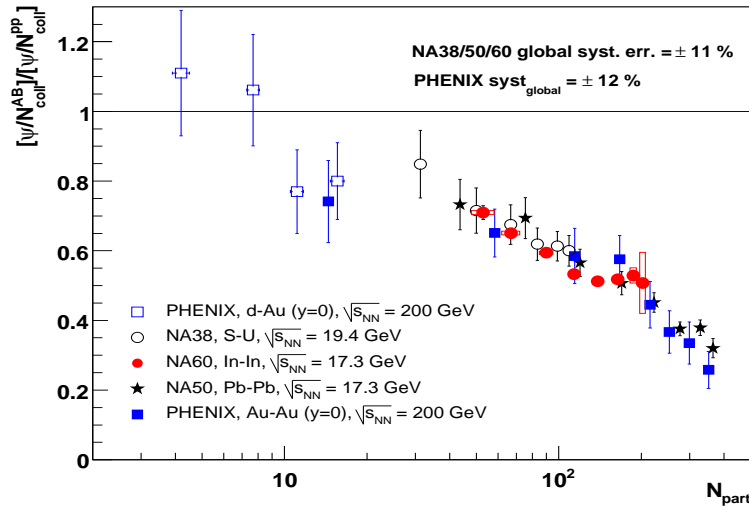

Figure 17. J/ψ nuclear modification factor versus centrality [190] (given by the number of participant nucleons in the collision) measured in *AA* and *p(d)A* collisions at SPS [186, 187, 188] and RHIC [71, 189].

Other explanations of the comparatively low depletion of J/ψ yields at RHIC have been put forward based on a much stronger direct J/ψ suppression (at temperatures close to T_{crit}) combined with $c\bar{c}$ pairs regeneration from the abundant charm quarks†† in the dense medium [192]. The LHC measurements will be crucial to resolve this issue. A strongly suppressed J/ψ yield in *PbPb* at 5.5 TeV – where the expected initial temperatures will be well above $2T_{crit}$ – would support the sequential-screening scenario, whereas recombination models predict a strong enhancement due to the larger density of $c\bar{c}$ pairs in the medium. In addition, the abundant production of the $\Upsilon(1s, 2s, 3s)$ states at LHC energies will open up a unique opportunity to study the threshold dissociation behaviour of the whole bottomonium family. The Υ is expected to survive up to $4T_{crit}$ and, therefore, *direct* suppression of the $b\bar{b}$ ground-state would be indicative of medium temperatures around 1 GeV at the LHC.

††10 charm pairs are produced on average in a central *AuAu* collision at the top RHIC energy.

11. Chiral symmetry restoration: In-medium vector mesons

In-medium modifications of the spectral function (mass, width) of the light vector mesons (ρ, ω, and ϕ) have been proposed as a promising signature of the (approximate) restoration of chiral symmetry in the u, d, s quark sector [38, 39]. In the QCD vacuum the spontaneous breaking of chiral symmetry manifests itself in the hadron spectrum through the mass-splitting of "chiral partners" i.e. between states of opposite parity but equal quantum numbers. Chiral symmetry breaking leads, in the mesonic sector, to the non-degeneracy of the pseudo-/scalar ($\pi - \sigma$) and axial-/vector ($a_1 - \rho$) channels. For temperatures above the chiral transition, massless left- and right-handed quarks will decouple and one expects to observe a gradual disappearance of the mass-splitting, leading to a shift of the masses of vector mesons and their chiral partners. The ρ meson is an excellent candidate for the experimental study of in-medium spectral functions in *AA* collisions due to (i) its short lifetime ($\tau_0 = 1.3$ fm/c) allowing it to decay before regaining its vacuum spectral shape, and (ii) its (rare but detectable) dilepton decay branching ratio ($\Gamma_{l+l-} \approx 5 \cdot 10^{-5}$) which is unaffected by final-state interactions with the surrounding environment.
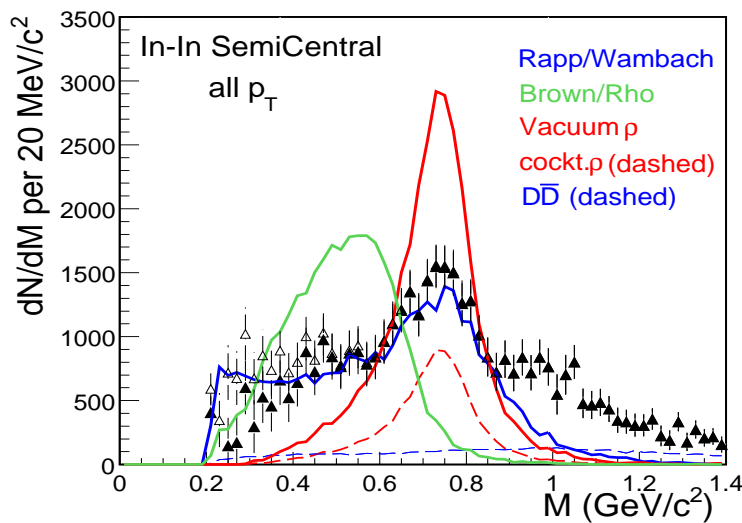

Figure 18. "Excess" invariant $\mu^+\mu^-$ mass spectrum in semi-central *InIn* collisions at $\sqrt{s_{NN}} = 17.3$ GeV [32] compared to the expected ρ line-shape in different theoretical scenarios: vacuum ρ, collisional broadening [38, 193], and mass drop [39].

The NA60 experiment has recently studied a high-statistics sample of low mass muon pairs in *InIn* collisions at $\sqrt{s_{NN}} = 17.3$ GeV [32]. The measured ρ spectrum, after subtraction of all other sources of opposite-sign muon pairs, is peaked at the nominal (free) mass ($m_\rho = 0.77$ GeV/c^2) but its width is substantially broadened for increasing centralities (Fig. 18). The ρ spectral shape is better reproduced by models which consider in-medium width broadening due to interactions in a hot and dense *hadronic* medium close to the expected phase boundary ($T \sim 190$ MeV) [193], than by a long-standing prediction based on a downwards mass-shift coupled directly to the melting of the chiral condensate [39]. Such a result sets new constraints

on the possible realization of chiral symmetry in QCD matter. At RHIC energies, the factor of two larger temperatures reached compared to SPS prefigure that the ρ should exhibit a completely "melted" line-shape if, as expected from the lattice, the chiral and deconfinement transitions occur at the same T_{crit}. The ρ measurement in the dielectron channel will be possible in PHENIX with the recently installed hadron-blind-detector [194] which will allow to suppress by two orders of magnitude the large combinatorial background arising from light-meson Dalitz decays and photon conversions, while preserving 50% of the signal.

Summary

High-energy collisions of heavy ions provide the only existing method today to explore empirically the phase diagram of QCD at extreme values of temperature, density and low-*x*. We have reviewed the experimental and phenomenological progress in nucleus-nucleus collisions at BNL-RHIC ($\sqrt{s_{NN}} \approx 20 - 200$ GeV) and CERN-SPS ($\sqrt{s_{NN}} \approx 20$ GeV) in recent years with a particular emphasis on the modifications suffered by different hard probes in the QCD medium that is produced, compared to baseline measurements in proton-proton or proton(deuteron)-nucleus collisions. The observed modifications allow us to obtain direct information on fundamental (thermo)dynamical properties of strongly interacting matter.

The reduced *AuAu* hadron multiplicities and the depleted yields of semihard hadrons ($p_T \approx 1 - 4$ GeV/*c*) at forward rapidities in *dAu* collisions indicate that the initial conditions of the nuclei accelerated at RHIC energies are consistent with Colour-Glass-Condensate approaches that model the hadronic parton distributions as a low-*x* saturated gluon wavefunction evolving according to non-linear QCD equations. These new data – complementary to the rich HERA results on the partonic structure of the proton – shed new light on the high-energy limit of QCD, a physics topic not only appealing in its own right but an essential ingredient for any serious attempt to compute a large variety of hadron-, photon- and neutrino- scattering cross sections at increasingly large energies.

The robust radial and elliptic flows seen for all identified hadron species up to $p_T \approx 2$ GeV/*c* in *AuAu* reactions at $\sqrt{s_{NN}} = 200$ GeV are remarkably well described by *ideal* relativistic hydrodynamics calculations which model the expanding system starting with a realistic QGP equation-of-state with initial energy densities $\varepsilon_0 \approx 30$ GeV/fm^3 at thermalization times $\tau_0 \approx 0.6$ fm/*c*. Detailed hydro-data comparisons for various differential observables – in particular the elliptic flow parameter $v_2(p_T)$ for different light and heavy hadron species – indicate that the system exhibits very small viscosities (i.e. very short mean free paths) and is strongly coupled at variance with the anticipated QGP paradigm of a weakly interacting gas of relativistic partons. In the intermediate $p_T \approx 2 - 4$ GeV/*c* range, baryons have enhanced yields and flows compared to mesons pointing to a novel channel for hadronization based on constituent-quark coalescence in a dense partonic medium. The existence of a new mechanism of hadron formation in heavy-ion reactions at transverse momenta of a few GeV/*c*, apart from standard parton fragmentation, offers new ways to probe the space-time dynamics of confinement in different

QCD environments.

In the high-p_T sector, leading hadrons (but not colour-blind prompt γ) are suppressed by up to a factor of $\sim$5 in the range $p_T \approx 4 - 20$ GeV/c compared to perturbatively-scaled proton-proton spectra. This result is in agreement with non-Abelian energy loss models that assume that the produced partons traverse a medium with very large parton rapidity densities $dN^g/dy \approx 1100$ and transport coefficients $\langle \hat{q} \rangle \approx 10$ GeV^2/fm. The energy lost by the quenched parton in the medium apparently shows up in a very unconventional conical-like azimuthal profile of secondary hadrons ($p_T \approx 1 - 3$ GeV/c) in the away-side hemisphere of high-p_T trigger hadrons. Interpretations of this preferential azimuthal emission at $\Delta\phi \approx \pi\pm$ 1.1, as caused by the generation of a Mach-cone boom by a supersonic parton propagating through the dense system, yield average speeds of sound $\langle c_s \rangle = \cos(\theta_M) \approx 0.45$ not far from those expected from lattice QCD for deconfined quark-gluon matter.

In the electromagnetic sector, preliminary real and virtual γ spectra in central *AuAu* in the range $p_T = 1 - 14$ GeV/c can be described as the sum of a perturbative (prompt) photon contribution plus a secondary component of thermal origin. Hydrodynamics calculations can reproduce the data assuming the formation of a radiating QGP with average temperatures $2T_{crit} \approx 350$ MeV. Such temperature values seem to be consistent with the observation that the amount of J/ψ suppression at RHIC and SPS is about the same as expected from lattice-based calculations that predict a survival of the $c\bar{c}$ ground state up to $T \approx 2T_{crit}$ but a "melting" of the χ_c and ψ' (which feed-down at a $\sim$40% level to the J/ψ) near T_{crit}. At the CERN SPS, recent NA60 results on the ρ spectral function in central *InIn* collisions at $\sqrt{s_{NN}} = 17.3$ GeV indicate that the width of the vector meson is substantially broadened in the medium. Theoretical calculations indicate that most of the broadening can be accounted for by collisional effects in a hot and dense hadronic medium with initial temperatures close to $T_{crit} \approx 175$ MeV (note that such a result is also consistent with the observed hadron abundances at SPS which indicate that the system reaches chemical equilibrium at temperatures around 160 MeV).

The overall scenario taking form from the wealth of recent experimental data suggests, on the one hand, that heavy-ion collisions at RHIC energies produce a strongly interacting liquid-like QGP with very large initial parton rapidity densities $dN^g/dy \approx 1100$, temperatures $2T_{crit} \approx$ 350 MeV and very low shear viscosities. On the other hand, systems produced at SPS seem to be only partially thermalised – according to the lower measured collective anisotropic flow compared to RHIC –, have initial $dN^g/dy \approx 400$ and temperatures around the phase boundary at $T_{crit} \approx 175$ MeV. However, it is fair to acknowledge that among the existing signals there is yet no incontrovertible "textbook" figure *proving* the formation of a thermalised extended medium consisting of deconfined and chirally-symmetric quarks and gluons. One such evidence would be a direct empirical observation of a jump in the number of effective degrees of freedom at the phase change as expected by EoS calculations in the lattice. Since RHIC top energies seem to produce systems at twice T_{crit} and SPS data point to conditions just at the predicted phase change, the expected jump is likely to be observed (e.g. via precise stud-

ies of the correlation of thermal photon slopes with the global hadron multiplicities) in a next phase of RHIC running at intermediate energies ($\sqrt{s_{NN}} \approx 20 - 62$ GeV) and high luminosities. Likewise, confirmation of the concurrent chiral and deconfinement transitions in QCD matter will require e.g. precise measurements of the ρ spectral shape (and, ideally, that of its chiral partner a_1) at RHIC energies. Lower-energy runs at RHIC, as well as at the projected CBM facility [195], will access also the region of large baryon densities around the QCD critical point. Finding signs of the tri-critical point at relatively high temperatures would indicate that the smooth cross-over changes to a first order phase transition at higher baryon densities, a result of relevance for the conditions prevailing in the core of neutron (and other compact) stars. Direct validation of the strongly-coupled interpretation of the medium formed at RHIC and potential observation of the anticipated *weakly* interacting quark-gluon plasma require key measurements in *PbPb* at 5.5 TeV at CERN-LHC where the initial temperatures $\mathcal{O}(1$ GeV$)$ should be large enough to observe the direct melting of ground-state quarkonia resonances. In addition, at the LHC, the longer duration of the QGP phase and the much abundant production of other hard probes (in particular parton energy loss results for *fully* reconstructed, γ- or Z-tagged, and flavour-identified jets) thermal photons, v_2 flow parameter, etc. will likely result in indisputable probes of the deconfined medium much less dependent on details of the later hadronic phase.

The experimental advances in the last years have been paralleled by significant progresses in the theoretical description of high-density QCD matter. Lattice methods are increasingly more refined and powerful to describe not only the infrared collective dynamics (EoS, critical parameters) but also the in-medium correlators (quarkonia). Effective field theories have been developed in specific domains such as the Colour-Glass-Condensate which effectively describes the high-energy (low-x) limit of QCD. Perturbative calculations have substantially improved the description of the interaction of hard probes with hot and dense quark-gluon matter. Last but not least, duality approaches based on the application of AdS/CFT correspondence between weakly coupled gravity and strongly coupled QCD-like systems, are providing new powerful insights on dynamical properties that cannot be directly treated by either perturbation theory or lattice methods while simultaneously opening novel directions for phenomenological studies and experimental searches.

The impressive experimental and theoretical advances triggered by the wealth of high-statistics, high-quality data collected in ultrarelativistic nucleus-nucleus collisions at RHIC and SPS, have significantly expanded the knowledge of many-body QCD at extreme conditions of temperature, density and low-x. Those studies – which will be substantially extended in the upcoming LHC (and likely RHIC-II) nucleus-nucleus and proton-nucleus programme – go beyond the strict realm of the strong interaction and shed light on a vast ramification of fundamental physics problems. Knowledge of the collective behaviour of many-parton systems is of primary importance not only to address basic aspects of the strong interaction such as the nature of confinement or the mechanism of mass generation via chiral symmetry breaking, but to ascertain the high-energy limit of all scattering cross sections

involving hadronic objects, the inner structure of compact stellar objects, or the evolution of the early universe between the electroweak transition and primordial nucleosynthesis.

Acknowledgments

References

[1] See e.g. Karsch F and Laermann E 2003 in Hwa R C (ed) *et al.* "QGP. Vol 3" 1-59, World Scientific

[2] Shuryak E V 1978 Sov. Phys. JETP **47** 212 [Zh. Eksp. Teor. Fiz. **74** 408]; also Collins J C And Perry M J 1975 *Phys. Rev. Lett.* **34** 1353, and Freedman B A and McLerran L D 1977 *Phys. Rev. D* **16** 1169

[3] Jaffe A M and Witten E 2000, "Quantum Yang-Mills Theory", Clay Maths Inst. Millennium Prize, http://www.claymath.org/millennium/Yang-Mills_Theory; and Gross D 2000, in "Ten Problems in Fundamental Physics", http://feynman.physics.lsa.umich.edu/strings2000/millennium.html

[4] Schaefer T 2005 "HUGS 2005 Lectures" World Scientific *Preprint* hep-ph/0509068

[5] Cleymans J, Oeschler H, Redlich K and Wheaton S 2006 *J. Phys* **G**32 S165

[6] Schwarz D J 2003, Ann. Phys. 12 220

[7] H1 Collaboration Adloff C *et al.* 2001 *Eur. Phys. J.* **C21** 33; ZEUS Collaboration Breitweg J *et al.* 1999 *Eur. Phys. J.* **C7** 609

[8] Gribov V N and Lipatov L N 1972, Sov. J. Nucl. Phys. **15** 438; Altarelli G and Parisi G 1977 *Nucl. Phys.* **B126** 298; Dokshitzer Yu L 1977, Sov. Phys. JETP **46** 641

[9] Lipatov L N 1976, Sov. J. Nucl. Phys. **23** 338; Kuraev E A, Lipatov L N and Fadin V S 1977, Zh. Eksp. Teor. Fiz **72** 3; Balitsky Ya Ya, Lipatov L N 1978, Sov. J. Nucl. Phys. **28** 822

[10] See e.g. Iancu E and Venugopalan R 2003 in Hwa R C (ed) *et al.* "QGP. Vol 3" 249-3363, World Scientific

[11] Jalilian-Marian J, Kovner A, Leonidov A and Weigert H 1997, *Nucl. Phys.* **B504** 415; Jalilian-Marian J, Kovner A, Leonidov A and Weigert H 1999, *Phys. Rev.* **D59** 014014; Iancu E, Leonidov A and McLerran L 2001 *Nucl. Phys.* **A692** 583;

[12] Kovchegov Y V 1999 *Phys. Rev.* **D60** 034008

[13] Maldacena J M 1998 Adv. Theor. Math. Phys. 2 231 [Int. J. Theor. Phys. 38 1113]; Witten E 1998 Adv. Theor. Math. Phys. 2 505

[14] Kovtun P, Son D T and Starinets A O 2005, *Phys. Rev. Lett.* **94** 111601

[15] Liu H, Rajagopal K and Wiedemann U A 2006 *Phys. Rev. Lett.* **97** 182301

[16] Herzog C P *et al.* 2006 JHEP **0607** 013, Gubser S S 2006 *Phys. Rev. D* **74** 126005, Casalderrey-Solana J and Teaney D 2006 *Phys. Rev.* **D74** 085012

[17] Rajagopal K and Wilczek F 2000 in Shifman M (ed.) "At the frontier of particle physics Vol. 3", 2061-2151; Alford M G, Rajagopal K and Wilczek F 1998 *Phys. Lett. B* **422** 247

[18] Schukraft J 2006 *Preprint* nucl-ex/0602014

[19] Bjorken J D 1983 *Phys. Rev.* **D27** 140

[20] PHENIX Collaboration Adler S S *et al.* 2005 *Phys. Rev.* **C**71 034908

[21] STAR Collaboration Sahoo R *et al.* 2006 *Rom. Rep. Phys.* **58** 055

[22] Kolb P F and Heinz U in Hwa R C (ed) *et al.* "QGP. Vol 3" 634-714, World Scientific

[23] Letessier J and Rafelski J 2000 *Int. J. Mod. Phys. E* **9** 107

[24] Antinori J 2004 *J. Phys. G* **30** S725

[25] Braun-Munzinger P, Redlich K and Stachel J 2003 in Hwa R C (ed) *et al.* "QGP. Vol 3", World Scientific;

[26] Lisa M A, Pratt S, Soltz R and Wiedemann U A 2005 Ann. Rev. Nucl. Part. Sci. **55** 357

[27] Jeon S and Koch V 2003 in Hwa R C (ed) *et al.* "QGP. Vol 3", World Scientific, 430-490

[28] PHENIX Collaboration Adcox K *et al.* 2005 *Nucl. Phys.* **A**757 184

[29] STAR Collaboration Adams J *et al.* 2005 *Nucl. Phys.* **A**757 102

[30] PHOBOS Collaboration Back B B *et al.* 2005 *Nucl. Phys.* **A**757 28

[31] BRAHMS Collaboration Arsene I *et al.* 2005 *Nucl. Phys.* **A**757 1

[32] NA60 Collaboration Arnaldi R *et al.* 2006 *Phys. Rev. Lett.* **96** 162302

[33] Azimov Y I , Dokshitzer Y L Khoze V A and Troian S I 1985 *Z. Phys. C* **27** 65

[34] Kharzeev D and Nardi N 2001 *Phys. Lett. B* **507** 121; Kharzeev D, Levin E and Nardi M 2005 *Nucl. Phys. A* **747** 609

[35] Baier R, Dokshitzer Y L, Mueller A H, Peigné S and Schiff D 1997 *Nucl. Phys.* **B484** 265; Baier R, Schiff D, Zakharov B G 2000 Ann. Rev. Nucl. Part. Sci. **50** 37

[36] Gyulassy M, Vitev I, Wang X N and Zhang B W 2003 in Hwa R C (ed.) *et al.*: "QGP. Vol. 3" 123-191 World Scientific, Kovner A and Wiedemann U A in Hwa R C (ed.) *et al.*: "QGP. Vol. 3" 192-248 World Scientific

[37] Matsui T and Satz H 1986 *Phys. Lett.* **B**178 416

[38] See e.g. Rapp R and Wambach J 2000 *Adv. Nucl. Phys.* **25** 1

[39] Brown G E and Rho M 2002, *Phys. Rept.* **363** 85

[40] Huovinen P and Ruuskanen P V 2006 *Ann. Rev. Nucl. Part. Sci.* **56**

[41] Hwa R C and Yang C B 2003 *Phys. Rev.* **C67** 034902; Fries R J, Muller B, Nonaka N and Bass S A 2003, *Phys. Rev.* **C68** 044902; Greco V, Ko C M and Levai P 2003 *Phys. Rev. Lett.* **90** 202302

[42] Stankus P 2005 Ann. Rev. Nucl. Part. Sci. **55** 517 and refs. therein

[43] Mangano M, Satz H and Wiedermann U "Hard probes in heavy-ion collisions at the LHC" CERN-2004-009 see detailed refs. [76, 144, 147, 184]

[44] Jacobs P and Wang X N 2005 *Prog. Part. Nucl. Phys.* **54** 443

[45] Collins J C, Soper D E and Sterman G 1985 *Nucl. Phys. B* **261** 104

[46] See e.g. d'Enterria D in CERN Yellow Report on Hard Probes in Heavy Ion Collisions at the LHC *Preprint* nucl-ex/0302016

[47] Hahn H *et al.* 2003 *Nucl. Instrum. Methods* **A** 499 245

[48] Fischer W *et al.* 2004 EPAC-2004-MOPLT165, Lucerne, Switzerland.

[49] BRAHMS Collaboration J. Adamczyk et.al. 2003 *Nucl. Instrum. Methods* **A499** 437

[50] PHOBOS Collaboration B. B. Back 2003 *Nucl. Instrum. Methods* **A499** 603

[51] PHENIX Collaboration Adcox K 2003 *et al. Nucl. Instrum. Methods* **A499** 469

[52] STAR Collaboration Ackermann K H *et al. Nucl. Instrum. Methods* **A499** 624

[53] Lourenço C 2006 *Czech. J. Phys.* **56** A13; NA60 Collaboration Usai G *et al.* 2005 *Eur. Phys. J.* **C**43 415

[54] Keil N *et al.* 2005 *Nucl. Instrum. Methods* **A565** 55

[55] STAR Collaboration Abelev B I *et al.* 2006 *Phys. Rev. Lett.* **97** 252001

[56] STAR Collaboration Adams J *et al.* 2003 *Phys. Rev. Lett.* **91** 172302

[57] PHENIX Collaboration Adler S S *et al.* 2003 *Phys. Rev. Lett.* **91** 241803

[58] PHENIX Collaboration Adler S S *et al.* 2007 *Phys. Rev. Lett.* **98** 012002

[59] PHENIX Collaboration Adare A *et al.* 2006 *Phys. Rev. Lett.* **97** 252002

[60] BRAHMS Collaboration Arsene I *et al.* 2004 *Phys. Rev. Lett.* **93** 242303

[61] STAR Collaboration Adams J *et al.* 2004 *Phys. Rev. Lett.* **92** 171801

[62] STAR Collaboration Abelev B I 2006 *Preprint* nucl-ex/0607012

[63] Aversa F *et al.* 1989 *Nucl. Phys. B* **327** 105, Jager B *et al.* 2003 *Phys. Rev. D* **67** 054005, and Vogelsang W (private communication)

[64] Gordon L E and Vogelsang W 1993 *Phys. Rev. D* **48** 3136, 1994 *Phys. Rev. D* **50** 1901, and Vogelsang W (private communication); Aurenche P *et al.* 1984 *Phys. Lett.* **B140** 87; and 1988 *Nucl. Phys.* **B297** 661

[65] Cacciari M, Nason P and Vogt R 2005 *Phys. Rev. Lett.* **95** 122001

[66] Pumplin J *et al.* 2002 JHEP **0207** 012

[67] Kniehl B A, Kramer G and Potter B 2001 *Nucl. Phys. B* **597** 337

[68] Kretzer S 2000 *Phys. Rev.* **D62** 054001

[69] Bourrely C and Soffer J 2004 *Eur. Phys. J. C* **36** 371

[70] Aurenche P *et al* 2006 *Phys. Rev. D* **73** 094007

[71] PHENIX Collaboration Adler S S *et al.* 2006 *Phys. Rev. Lett.* **96** 012304

[72] PHENIX Collaboration Adler S S *et al.* 2003, *Phys. Rev. Lett.* **91** 072303; PHENIX Collaboration Adler S S *et al.* 2006 *Preprint* nucl-ex/0610036

[73] Vogt R 2005 *Phys. Rev. C* **71** 054902

[74] Guzey V, Strikman M and Vogelsang W 2004 *Phys. Lett. B* **603** 173

[75] Eskola K J, Kolhinen V J and Salgado C 1999 *Eur. Phys. J. C* **9** 61

[76] Accardi A *et al.* "Hard probes in heavy ion collisions at the LHC: PDFs, shadowing and *pA* collisions" *Preprint* hep-ph/0308248

[77] Cronin J W *et al.* 1975 *Phys. Rev.* D**11** 3105; Antreasyan D *et al.*1979 *Phys. Rev.* **D19** 764

[78] Gyulassy M and Wang X N 1994 *Comput. Phys. Commun.* 83, 307

[79] Capella A, Sukhatme U, Tan C I and Tran Thanh Van J 1994 *Phys. Rept.* **236** 225

[80] Armesto N and Pajares C 2000 *Int. J. Mod. Phys. A* **15** 2019

[81] Eskola K J 2002 *Nucl. Phys. A* **698** 78

[82] Armesto N, Salgado C A and Wiedemann U A 2005 *Phys. Rev. Lett.* **94** 022002

[83] Gribov L V, Levin E M and Ryskin M G 1983 *Phys. Rept.* **100** 1

[84] Mueller A H and Qiu J w 1986 *Nucl. Phys. B* **268** 427

[85] McLerran L D and Venugopalan R 1994 *Phys. Rev. D* **50** 2225, Phys. Rev. D **49** 3352, Phys. Rev. D **49** 2233

[86] Accardi A 2005 *Acta Phys. Hung. A* **22** 289

[87] de Florian D and Sassot R 2004 *Phys. Rev. D* **69** 074028

[88] Kharzeev D, Kovchegov Y and Tuchin K 2004 *Phys. Lett. B* **599** 23

[89] Jalilian-Marian J 2005 *Nucl. Phys. A* **748** 664

[90] Dumitru A, Hayashigaki A and Jalilian-Marian J 2006, *Nucl. Phys. A* **765** 464

[91] d'Enterria D 2007 *Eur. Phys. J.* **C49** 155

[92] d'Enterria D and Peressounko D 2006, *Eur. Phys. J. C* **46** 451

[93] Ollitrault J Y 1992 *Phys. Rev. D* **46**, 229

[94] Voloshin S and Zhang Y 1996 *Z. Phys. C* **70** 665

[95] Kolb P F, Sollfrank J and Heinz U W 2000 *Phys. Rev. C* **62** 054909

[96] Akiba Y [PHENIX Collaboration] 2006 *Nucl. Phys. A* **774** 403

[97] Snellings R 2005 *AIP Conf. Proc.* **756** 390

[98] PHOBOS Collaboration Manly S *et al.* 2006 *Nucl. Phys. A* **774** 523

[99] PHENIX Collaboration Adare A *et al* 2006 *Preprint* nucl-ex/0608033

[100] Zhu X I, Bleicher M and Stoecker H 2005 *Phys. Rev.* **C72** 064911

[101] Molnar D and Gyulassy M 2002 *Nucl. Phys.* **A697** 495 [Errat.-ibid. A **703** 893]

[102] Teaney D, Lauret J and Shuryak E V 2001 *Preprint* nucl-th/0110037

[103] Hirano T and Tsuda K 2002 *Phys. Rev.* **C66** 054905

[104] NA49 Collaboration Alt C *et al.* 2003 *Phys. Rev.* **C68** 034903

[105] Voloshin S A 2006 *AIP Conf.Proc.* 870 691

[106] PHENIX Collaboration Adler S S *et al.* 2005 *Phys. Rev. Lett.* **94** 232302

[107] PHENIX Collaboration Adcox K *et al.* 2002 *Phys. Rev. Lett.* **89** 212301

[108] Voloshin S A and Poskanzer A M 2000 *Phys. Lett.* **B474** 27

[109] Teaney D 2003 *Phys. Rev.* **C68** 034913

[110] Hirano T and Gyulassy M 2006 *Nucl. Phys.* **A769** 71

[111] Moore G D and Teaney D 2005 *Phys. Rev.* **C71** 064904

[112] van Hees, Greco V and Rapp R 206 *Phys. Rev.* **C**73 034913

[113] Shuryak E V 2004 *Prog. Part. Nucl. Phys.* **53** 273

[114] Lee T D 2005 *Nucl. Phys.* **A750** 1

[115] Gyulassy M and McLerran L 2005 *Nucl. Phys.* **A750** 30

[116] Peshier A and Cassing W 2005 *Phys. Rev. Lett.* **94** 172301

[117] Heinz U W 2005 *Preprint* nucl-th/0512051

[118] Thoma M H 2005 *J. Phys* **G31** L7

[119] Cheng M *et al.* 2006 *Phys. Rev.* **D**74 054507

[120] PHENIX Collaboration Adcox K *et al.* 2002 *Phys. Rev. Lett.* **88** 022301; STAR Collaboration Adler C *et al.* 2002 *Phys. Rev. Lett.* **89** 202301; PHENIX Collaboration Adler S S *et al.* 2003 *Phys. Rev. Lett.* **91** 072301

[121] Bjorken J D 1982 FERMILAB-PUB-82-059-THY

[122] Gyulassy G and Plümer M 1990 *Phys. Lett.* **B243** 432; Wang X N and Gyulassy M 1992 *Phys. Rev. Lett.* **68** 1480

[123] PHENIX Collaboration Adler S S *et al.* 2006 *Phys. Rev. Lett.* **96** 202301; Shimomura M [PHENIX Collaboration] 2006 *Nucl. Phys.* **A774** 457

[124] d'Enterria D 2004 Phys. Lett. B **596**, 32

[125] WA98 Collaboration Aggarwal M M *et al.* 2002 *Eur. Phys. J.* **C23** 225

[126] NA57 Collaboration Antinori *et al.* 2005 *Phys. Lett.* **B623** 17

[127] Blume C 2007 *Nucl. Phys.* **A783** 65

[128] PHENIX Collaboration Adler S S *et al.* 2005 *Phys. Rev. Lett.* **94** 232301

[129] Gyulassy M, Levai P and Vitev I 2000 *Phys. Rev. Lett.* **85** 5535; 2001 *Nucl. Phys.* **B594** 371

[130] Vitev I and Gyulassy M 2002 *Phys. Rev. Lett.* **89** 252301

[131] Wiedemann U A 2000 *Nucl. Phys.* **B588** 30; Salgado C A and Wiedemann U A 2003 *Phys. Rev.* **D68** 014008

[132] Zakharov B G 1997 JETP Lett. **65** 615;

[133] Djordjevic M, Gyulassy M and Wicks S 2005 *Phys. Rev. Lett.* **94** 112301; Wicks S, Horowitz S, Djordjevic M and Gyulassy M 2005 *Preprint* nucl-th/0512076

[134] Dainese A, Loizides C and Paic G 2005 *Eur. Phys. J.* **C38** 461

[135] Eskola K J, Honkanen H, Salgado C A Wiedemann U A 2005 *Nucl. Phys.* **A747** 511

[136] Armesto N, Dainese A, Salgado C A and Wiedemann U A 2005 *Phys. Rev.* **D71** 054027; Armesto N *et al.* 2006 *Phys. Lett.* **B637** 362

[137] Loizides C 2007 *Eur. Phys. J.* **C49** 339

[138] d'Enterria D 2005 *Eur. Phys. J.* **C43** 295

[139] PHENIX Collaboration Adler S S *et al.* 2006 *Phys. Rev. Lett.* **96** 032301

[140] Dokshitzer and Y L and Kharzeev D E 2001 *Phys. Lett.* **B519** 199

[141] Wang Q and Wang X N 2005 *Phys. Rev.* **C**71 014903

[142] Mustafa M G and Thoma M H 2005 *Acta Phys. Hung. A* **22** 93

[143] Peshier A 2007 *Eur. Phys. J.* **C49** 9

[144] Accardi A *et al.* "Hard probes in heavy ion collisions at the LHC: Jets" *Preprint* hep-ph/0310274

[145] Arleo F *et al.* 2004 JHEP **0411** 009

[146] Lokhtin I P, Sherstnev A V and Snigirev A M 2004 *Phys. Lett.* **B599** 260

[147] Bedjidian M *et al.* "Hard probes in heavy ion collisions at the LHC: Heavy Quarks" *Preprint* hep-ph/0311048

[148] Dainese A 2007 *Nucl. Phys.* **A783** 417

[149] See e.g Blazey G C *et al.* 2000 *Preprint* hep-ex/0005012

[150] STAR Collaboration Adler C *et al.* 2003 *Phys. Rev. Lett.* **90** 082302

[151] STAR Collaboration Adams J *et al.* 2005 *Phys. Rev. Lett.* **95** 152301

[152] PHENIX Collaboration Adler S S *et al.* 2006 *Phys. Rev. Lett.* **97** 052301

[153] Ajitanand N N *et al.* 2005 Phys. Rev. C **72** 011902

[154] STAR Collaboration Adams J *et al.* 2006 *Phys. Rev. Lett.* **97** 162301

[155] Peitzmann T [STAR Collaboration] 2006 Proceeds. Hard Probes'06.

[156] Polosa A D and Salgado C A 2006 *Preprint* hep-ph/0607295

[157] Stoecker H 2005 *Nucl. Phys.* **A750** 121

[158] Casalderrey-Solana J, Shuryak E and Teaney D 2005 *J. Phys. Conf. Ser.* **27** 22

[159] Ruppert J and Muller B 2005 *Phys. Lett.* **B618** 123

[160] Koch V, Majumder A and Wang X N 2006 *Phys. Rev. Lett.* **96** 172302

[161] Dremin I M 2006 Nucl. Phys. A **767** 233

[162] Mohanty B and Alam J e 2003 *Phys. Rev. C* **68** 064903

[163] Lacey R A 2006 *Preprint* nucl-ex/0608046.

[164] v Leeuwen M 2007 *Nucl. Phys.* **A783** 109

[165] Ajitanand N N 2007 *Nucl. Phys.* **A783** 519

[166] PHENIX Collaboration Adler S S *et al.* 2003 *Phys. Rev. Lett.* **91** 172301

[167] PHENIX Collaboration Adler S S *et al.* 2004 *Phys. Rev.* **C69**, 034910

[168] STAR Collaboration Adams J *et al.* 2006 *Phys. Rev. Lett.* **97** 152301

[169] STAR Collaboration Adams J *et al.* 2004 *Phys. Rev. Lett.* **92** 052302

[170] Tannenbaum M J 2006 Rept. Prog. Phys. **69** 2005 and refs. therein

[171] STAR Collaboration Adams J *et al.* 2006 *Phys. Lett.* **B637** 161

[172] PHENIX Collaboration Adler S S *et al.* 2003 *Phys. Rev. Lett.* **91** 182301

[173] STAR Collaboration Adams J *et al.* 2005 *Phys. Rev.* **C72** 014904

[174] Issah M and Taranenko A [PHENIX Collaboration] *Preprint* nucl-ex/0604011

[175] Molnar D and Voloshin S A 2003 *Phys. Rev. Lett.* **91** 092301

[176] Baier R, Mueller A H, Schiff D and Son D T 2001 *Phys. Lett.* **B502** 51

[177] Renk T, Bass S A and Srivastava D K 2005 *Phys. Lett.* **B632** 632

[178] Bathe S [PHENIX Collaboration] 2006 *Nucl. Phys.* **A774** 731

[179] Rasanen S S 2003 *Nucl. Phys.* **A715** 717

[180] Srivastava D K and Sinha B 2001 *Phys. Rev.* **C64** 034902; Srivastava D K 2001 Pramana **57** 235

[181] Turbide S, Rapp R and Gale C 2004 *Phys. Rev.* **C69** 014903

[182] Alam J e, Sarkar S, Hatsuda T, Nayak T K and Sinha B 2001 *Phys. Rev.* **C63** 021901

[183] d'Enterria D and Peressounko D 2007, in preparation

[184] Arleo F *et al.* 2003 in CERN Yellow Report on Hard Probes in Heavy Ion Collisions at the LHC *Preprint* hep-ph/0311131.

[185] Umeda T, Nomura K and Matsufuru H 2005 *Eur. Phys. J.* **C39S1** 9, Asakawa M and Hatsuda T 2004 *Phys. Rev. Lett.* **92** 012001 Datta S, Karsch F, Petreczky P and Wetzorke I 2004 *Phys. Rev.* **D69** 094507, Mocsy A and Petreczky P 2005 *Eur. Phys. J.* **C43** 77

[186] NA38 Collaboration Baglin C *et al.* 1995 *Phys. Lett.* **B345** 617

[187] NA50 Collaboration Abreu M C *et al.* 2000 *Phys. Lett.* **B477** 28

[188] NA60 Collaboration Arnaldi R *et al.* 2006 *Nucl. Phys.* **A774** 711

[189] PHENIX Collaboration A. Adare *et al.* 2006 *Preprint* nucl-ex/0611020

[190] Lourenço C 2007 *Nucl. Phys.* **A783** 451

[191] Karsch F, Kharzeev D and Satz H 2006 *Phys. Lett.* **B637** 75; Satz H 2007 *Nucl. Phys.* **A783** 249

[192] Thews R L, Schroedter M and Rafelski J 2001 *Phys. Rev.* **C63** 054905; Grandchamp L and Rapp R 2002 *Nucl. Phys.* **A709** 415

[193] van Hees H and Rapp R 2006 *Phys. Rev. Lett.* **97** 102301

[194] Fraenkel Z *et al.* 2005 *Nucl. Instrum. Methods* **A546** 466

[195] Friese V 2006 *Nucl. Phys.* **A774** 377